ISSN (print): 1698-6180. ISSN (online): 1886-7995
www.ucm.es/info/estratig/journal.htm

Journal of Iberian Geology 36 (1) 2010: 87-106

Journal of Iberian Geology
AN INTERNATIONAL PUBLICATION OF EARTH SCIENCES

Sand provenance and implications for paleodrainage in a rifted basin: the Tera Group (N. Spain)

Procedencia de areniscas e implicaciones en el paleodrenaje de una cuenca de rift: el Grupo Tera (N. España)

L. González-Acebrón[1]*, J. Arribas[2], R. Mas[1]

[1]Dto. Estratigrafía, Facultad de Ciencias Geológicas, Universidad Complutense de Madrid - Instituto de Geología Económica (CSIC-UCM), C/ José Antonio Nováis 2, 28040 Madrid (Spain)
[2]Dto. Petrología y Geoquímica, Facultad de Ciencias Geológicas, Universidad Complutense de Madrid - Instituto de Geología Económica (CSIC-UCM), C/ José Antonio Nováis 2, 28040 Madrid (Spain)

**Corresponding author: lgcebron@geo.ucm.es*

Received: 15/12/09 / Accepted: 05/02/10

Abstract

Fluvial-fan and fluvial siliciclastic strata, developed during the rifting that generated the Cameros Basin (North Spain), record important provenance changes that reveal source areas compositions and locations, paleodrainage evolution and rift patterns.

The Tera Group represents the first rifting stage in the Cameros Basin, containing fluvial-fan sediments at the lower part of the sedimentary fill that evolve to fluvial and lacustrine systems in the upper part of the record. Our quantitative sandstone petrographic analysis evidences the presence of three main petrofacies related closely to the rift basin evolution.

At the base of the sedimentary succession, Petrofacies 1 (quartzolithic) indicates that the fluvial-fans source areas included Jurassic marine carbonates and older siliciclastic Mesozoic units, as well as metamorphic supplies from the West Asturian Leonese Zone (WALZ).

Variscan basement sources of this metamorphic area (WALZ) were more abundant in the upper fluvial record (Petrofacies 2, quartzofeldspathic). Further, the influence of plutonic source areas with a mixed potassic and calcium-sodium composition is also recorded, probably related to the Central Iberian Zone (CIZ). In addition, a local sedimentary input was active during the fluvial

and lacustrine stages (Petrofacies 2 and 3, both quartzofeldspathic), as a function of the palaeogeographical position of the Jurassic marine rocks and the level of erosion reached. Plutonic rock fragments have not been observed in the Tera Group sandstones of the western part of the basin. Thus, deeper erosion of the basement in the eastern Cameros Basin is suggested.

The provenance evolution from quartzolithic to quartzofeldspathic petrofacies registered in Tera Group siliciclastic deposits is due to the higher influence of transversal supplies during the fluvial-fan stage (quartzolithic) to more important axial inputs during the fluvial stage (quartzofeldspathic). This provenance change represents the evolution from an undissected rift shoulder stage to more advanced stages of rifting (dissected rift shoulder) and during the beginning of a provenance cycle in a rifted basin.

Keywords: sandstone provenance, depositional sequences, rifted basin, Cameros Basin

Resumen

Los sedimentos de abanicos fluviales y fluviales propiamente dichos desarrollados durante el proceso de rift que generó la Cuenca de Cameros (Norte de España) registraron importantes cambios de procedencia que proporcionan información sobre la composición y localización de sus áreas fuente, la evolución del paleodrenaje y los patrones de rift.

Este estudio se centra en el Grupo Tera (Tithoniense) en el sector oriental de la Cuenca de Cameros. El Grupo Tera representa el primer estadio de rift en dicha cuenca, y está constituido por sedimentos de abanicos fluviales en la parte inferior del relleno sedimentario, que evolucionan a sistemas fluviales y lacustres hacia la parte superior del registro. El estudio petrográfico cuantitativo de las areniscas indica la presencia de tres petrofacies principales que muestran una estrecha relación con la evolución del rift.

En la base del registro sedimentario, la Petrofacies 1 (cuarzolítica) manifiesta que las áreas fuente de los abanicos fluviales incluyen tanto carbonatos Jurásicos marinos como unidades siliciclásticas mesozoicas previas, así como influencias metamórficas de la Zona Asturoccidental Leonesa (WALZ).

Los aportes del basamento varisco procedentes de esta área fuente metamórfica (WALZ) fueron más importantes en la parte alta del registro (Petrofacies 2, cuarzofeldespática). Además, se detecta la influencia de áreas fuente plutónicas con una composición mixta (potásica y calcosódica), probablemente relacionadas con la Zona Centroibérica (CIZ). También existió un aporte sedimentario local durante los estadios fluviales y lacustres (Petrofacies 2 y 3, ambas cuarzofeldespáticas), que tuvo lugar en función de la posición paleogeográfica de las rocas marinas Jurásicas y del nivel de erosión alcanzado.

Si comparamos los dos sectores de la cuenca, los fragmentos de roca plutónica no han sido observados en las areniscas del Grupo Tera en el sector occidental de la cuenca. Por lo tanto, se deduce un nivel de erosión del basamento más profundo en el sector occidental.

La evolución de la procedencia desde petrofacies cuarzolíticas a petrofacies cuarzofeldespáticas registrada en los depósitos siliciclásticos del Grupo Tera se debe a una mayor influencia de los aportes transversales durante la sedimentación de los abanicos fluviales (cuarzolíticos) hacia una mayor influencia de aportes axiales durante la etapa fluvial (cuarzofeldespática). Esta variación en la procedencia representa la evolución desde un estadio de hombrera de rift no erosionada a estadios más avanzados del rifting (hombrera de rift erosionada) y el comienzo de un ciclo de procedencia en una cuenca de rift.

Palabras clave: procedencia de areniscas, secuencias deposicionales, cuenca de rift, Cuenca de Cameros

1. Introduction

Sandstone petrography is widely considered to be a powerful tool for tectonic reconstructions and for determining the origin of ancient terrigenous deposits (Blatt, 1967; Dickinson, 1970; Pettijohn *et al.*, 1972). Many factors, such as source rocks, relief, climate and diagenesis affect the final sandstone composition. In areas of intense tectonic activity, source-rock type determines sediment composition more than do climate and relief (Dickinson, 1970). Several authors have described a relationship between the detrital composition of sandstones and the tectonic setting (e.g. Ingersoll, 1978; Dickinson and Suczek, 1979; Dickinson *et al.*, 1983; Dickinson, 1985; Valloni, 1985).

Multi-phase rifting and tilted crustal blocks lead to erosion and sediment redistribution within the basin, such that detrital modes of syn-rift sandstones strongly vary in relation to their paleotectonic position in the basin (e.g. Arribas *et al.*, 2003). The first stage of rifting usually starts with erosion of the pre-rift sedimentary substratum, followed by unroofing of the basement, constituting a provenance cycle (Arribas *et al.*, 2007). Thus, sandstone provenance studies are essential for reconstructing eroded strata and the tectonic evolution of rift basins (eg. Garzanti *et al.*, 2001 and 2003, Arribas *et al.*, 2003).

Sandstone provenance also helps to constrain the scale and pattern of ancient drainage (i.e. Tyrell *et al.*, 2007), and it is a key tool in facies prediction and paleogeographic reconstructions. The provenance study is used here to explore rift basin evolution and drainage patterns during the rift process.

In this paper, we compare the usefulness of different ternary diagrams and indices and their application to rift-

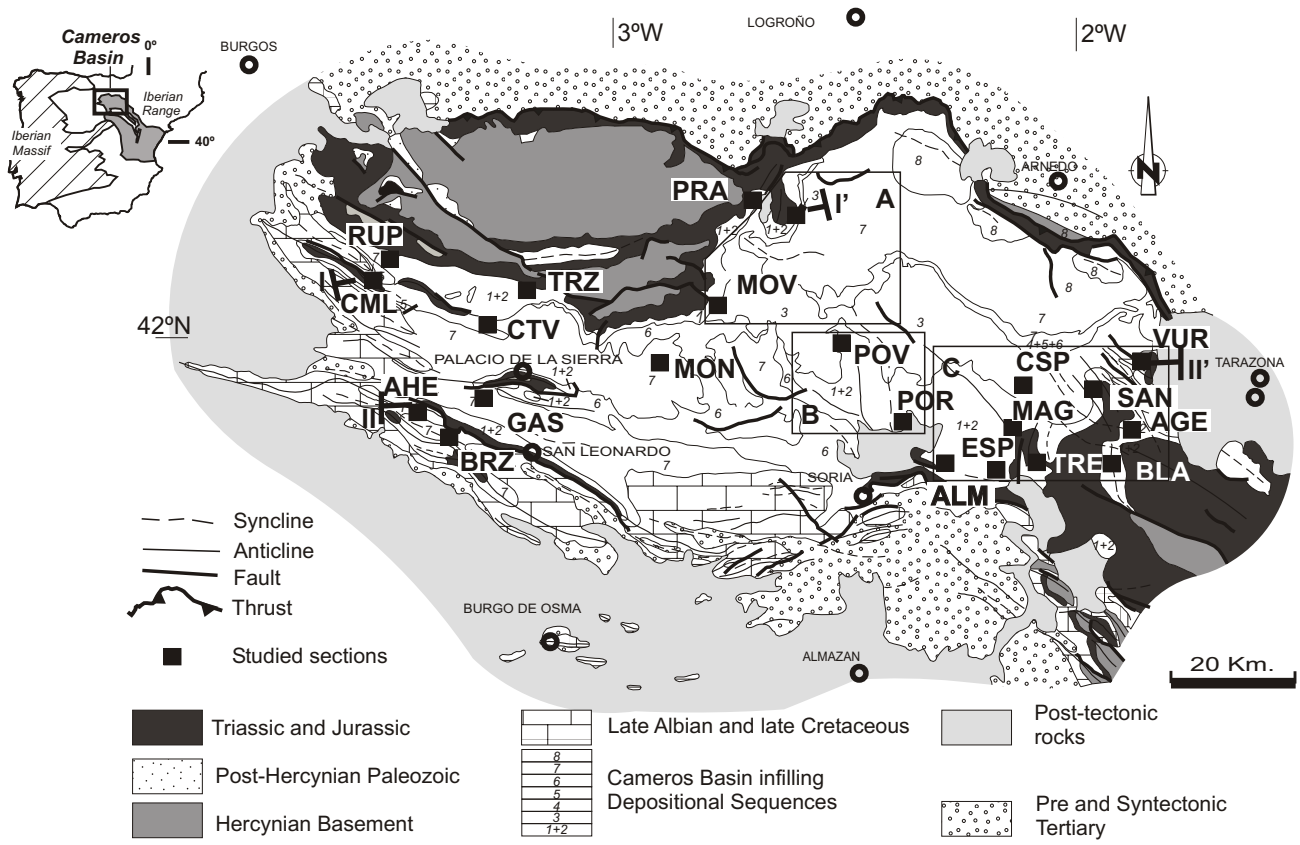

Fig. 1.- Geological map of the Cameros Basin indicating the location of the stratigraphic sections. Western part: MOV, Montenegro-Villoslada en Cameros; PRA: Pradillo; ALMA: Almarza; POV: La Póveda; POR: Portelrubio; ALM, Almajano; ESP: El Espino; MAG: Magaña; TRE: Trévago; CSP: El Collado de San Pedro Manrique; AGE: Ágreda; BLA: San Blas. Eastern part (samples from Arribas *et al.*, 2003): RUP: Rupelo; CML: Campolara; GAS: La Gallega; AHE: Arroyo del Helechal; BRZ: Brezales; CTV: Castrovido; TRZ: Terrazas; MON: Moncalvillo. A, B, C. Northern, central and southern parts of the study area, respectivelly. Modified from Mas *et al.*, 2002.

Fig. 1.- Mapa geológico de la Cuenca de Cameros indicando la posición de las secciones estratigráficas. Sector Oeste: MOV, Montenegro-Villoslada en Cameros; PRA: Pradillo; ALMA: Almarza; POV: La Póveda; POR: Portelrubio; ALM, Almajano; ESP: El Espino; MAG: Magaña; TRE: Trévago; CSP: El Collado de San Pedro Manrique; AGE: Ágreda; BLA: San Blas. Sector Este: (muestras de Arribas *et al.*, 2003): RUP: Rupelo; CML: Campolara; GAS: La Gallega; AHE: Arroyo del Helechal; BRZ: Brezales; CTV: Castrovido; TRZ: Terrazas; MON: Moncalvillo. A. Partes norte, central y sur de la zona de estudio, respectivamente. Modificada de Mas *et al.*, 2002.

ed basins, or more generally, in sandstones derived from sedimentary and metamorphic/plutonic source rocks. In our studied case, sedimentary source areas include both carbonate rocks and siliciclastic rocks. Most significant compositional variations among sandstones can be displayed as ternary plots on triangular diagrams. The three poles represent recalculated proportions of key categories of grain types determined by modal point counts. Such ternary diagrams do not adequately represent the vertical composition variations. This temporal evolution can be reflected in two-variable plots. Thus, we have selected some petrographic indices that represent properly the provenance cycles in rifted systems and evaluate the possible correlations between them.

Arribas *et al.* (2003) characterized the basin-fill successions of the western part of the Cameros Basin (see Fig. 1 for location) in terms of their clastic constituents and sandstone sources. These authors identified four main petrofacies (A, B, C and D) within seven depositional sequences in the basin (DS 1-DS 7, see Fig. 2). Petrofacies A and C are quartzosedimentolithic and characterize DS 1 and DS 4, respectively. These petrofacies record the erosion of Mesozoic pre-rift cover, mainly marine Jurassic deposits. Petrofacies B and D are quartzofeldspathic and are derived from the erosion of metamorphic terranes of the West-Asturian Leonese Zone during the deposition of DS 2 and DS 3, and to the erosion of coarse crystalline plutonic rocks from the Central Iberian Zone during DS 4 to DS 7, respectively. The present paper is focused on the Tera Group, which records the beginning of a continental rifting in the eastern Cameros Basin, and includes a comparison with previously described petrofacies evolution in the western sector of the basin.

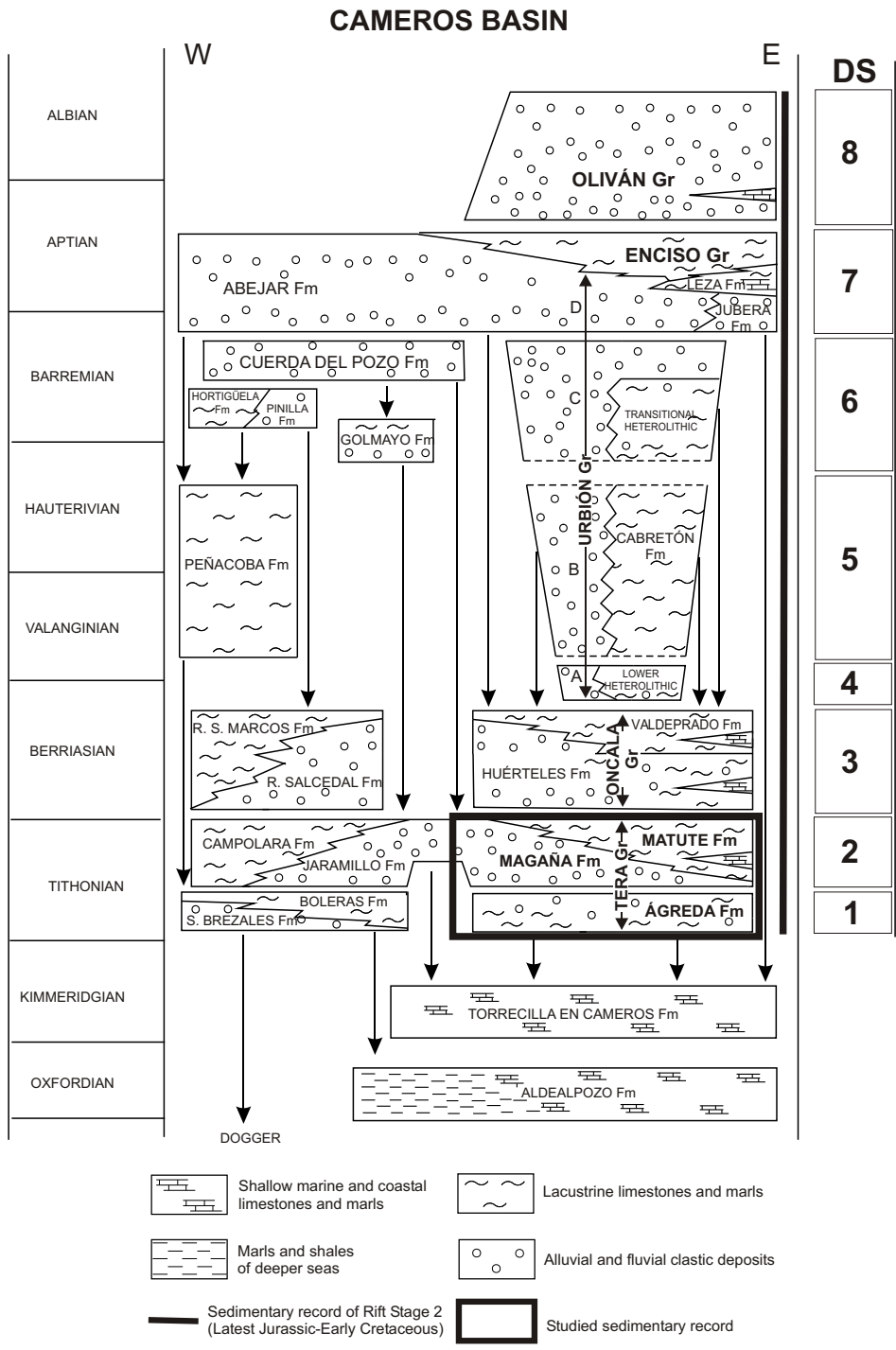

Fig. 2.- Stratigraphy of the depositional sequences (DS) of the Cameros Basin. The stratigraphic interval examined is indicated (Tera Group, DS 1 and DS 2). Modified from Mas *et al.*, 2004.

Fig. 2.- Estratigrafía de las secuencias deposicionales (SD) de la Cuenca de Cameros. El intervalo estratigráfico estudiado está indicado (Grupo Tera, SD 1 y SD 2). Modificada de Mas *et al.*, 2004.

The principal aims of this paper are: (1) To describe and discuss sandstone petrography interpreted to be representative of the beginning of a continental rifting; (2) to constrain the scales of drainage in the basin, with implications for the depositional setting; (3) to shed new light on the drainage orientation and source location; (4) to demonstrate major drainage reorganization driven by a change in rift style using provenance data; (5) to propose some petrographic indices that represent properly the compositional supply variations in rifted basins; (6) to contribute to a global data base of petrographic provenance data for intra-plate rift basins, which will help in making predictions on detrital-mode trends in space and time.

2. Geological and stratigraphic setting

The Cameros Basin in the northern Iberian Range (Fig. 1) forms part of the Mesozoic Iberian Rift System (Mas *et al.*, 1993; Guimerà *et al.*, 1995; Salas *et al.*, 2001; Mas *et al.*, 2002; Mas *et al.*, 2003). Intraplate rifting was a consequence of the opening of the oceanic Bay of Bis-

cay, which separated Iberia from Europe. The Cameros Basin is the westernmost basin of the Mesozoic Iberian Rift System.

The basin-fill succession of the Cameros Basin embodies a major cycle or megasequence composed of up to 6000 m of strata deposited from the Tithonian to Early Albian. These deposits overlie Upper Jurassic marine strata and are separated from them by an erosional unconformity with associated paleosols and/or paleokarst features (Alonso and Mas 1990; Benito, 2001, Benito *et al.*, 2001; Benito and Mas 2002).

The sedimentary infill of the Cameros Basin has been divided into eight depositional sequences (Mas *et al.*, 2002; Mas *et al.*, 2003) spanning the Tithonian to the Early Albian (Fig. 2). This sedimentary record consists of continental strata deposited by alluvial and lacustrine systems, with rare marine incursions (Mas *et al.*, 1993; Gómez Fernández and Meléndez, 1994). The Tera Group represents the first stage of rifting and is composed of two depositional sequences (DS 1 and DS 2, Fig. 2), which are Tithonian in age (Mas *et al.*, 1993; Mas *et al.*, 2004; Martín-Closas and Alonso Millán, 1998).

In the eastern Cameros basin, the Tera Group can be divided into three formations: Ágreda, Magaña and Sierra de Matute (Mas *et al.*, 1993; Gómez-Fernández and Meléndez, 1994) (Fig. 2). The main sedimentological characteristics of DS 1 and DS 2 in this sector are summarized as follows:

2.1. Depositional sequence 1

Ágreda Fm. The Ágreda Fm. is as much as 260 m thick with a depocenter area located to the south, near San Blas (BLA in Fig. 1). Two different types of lithosomes have been recognized in this formation: clastic lithosomes were deposited in fluvial-fans, as can be deduced from the radial facies distribution and grain size (Fig. 3). The fluvial-fans are related to the onset of rifting. A high rate of vertical accretion is indicated by a high ratio of floodplain to channel facies (eg: Shanley and McCabe, 1995). The paleocurrent analysis of these fluvial-fans was performed by Gómez Fernández and Meléndez, (1994), indicating sediment dispersal from the SE and SW of the study area. The second type of lithosome is represented by lacustrine and palustrine carbonate deposits and are restricted to the northern part of the study area (Fig. 3).

2.2. Depositional sequence 2

Magaña Fm. This formation is composed of channel-fill (sandy point-bars) and crevasse deposits, interbedded with floodplain mudstones displaying abundant paleosols. Sandstones occur generally as sheets of less than 5 m thick. The Magaña Fm. was deposited in a meandering fluvial system, more distal at the top of the sections (Fig. 4). The thickness of Magaña Fm. reaches 700 m in the depocenter area, located in the southern part of the study area (SAN, Fig. 1). A secondary depocenter has been recognized in the northern part of the study area (ALMA, Fig. 1). Sediment dispersal patterns of the meandering fluvial systems have been interpreted as NNW towards SSE of the study area (González-Acebrón, 2009).

Sierra de Matute Fm. This formation is less than 660 m thick, and its depocenter is located to the southern part of the study area (SAN, Fig. 1). Three stages of lacustrine depositional environments have been differentiated in this formation (González-Acebrón, 2009): (1) Shallow carbonate-producing lakes and shallow lakes with mixed carbonate and siliciclastic sedimentation; (2) shallow ephemeral alkaline lakes with common stromatolites and evaporite pseudomorphs; (3) shallow carbonate lakes rich in organic matter, restricted to the south area of the eastern Cameros Basin.

Fluvial and lacustrine systems could be partially coeval and interconnected. The clastic sedimentation in the lakes was probably related with the meandering fluvial systems of the Magaña Fm., which discharged into the lake systems.

3. Methods

Ninety six samples of medium-grained sandstones were collected from 15 representative stratigraphic sections of the Tera Group (see Fig. 1 for locations), in which the three formations of the Tera Group are globally well represented. The stratigraphic sections of the Eastern Tera Group were correlated to 8 stratigraphic sections of the western Tera Group (data from Arribas *et al.*, 2003) (Figs. 5 and 6). Thin sections were etched and stained using HF and sodium cobaltinitrite for potassium feldspar, and alizarin-red and potassium ferrocyanide for carbonate identification (methods of Chayes, 1952, and Lindholm and Finkelman, 1972, respectively). To characterize detrital modes, quantitative petrographic analysis was performed on thin sections by the integrated "Gazzi-Zuffa" point counting method (Gazzi, 1966; Zuffa, 1985). This procedure combines the "Gazzi-Dickinson" and traditional criteria (Ingersoll *et al.*, 1984). Four hundred to four hundred and fifty points were counted per slide. Post-depositional modifications of the original framework (e.g. feldspar replacement) were assessed to reconstruct the original composition of the sandstone framework. The petrographic data (Tables 1 and 2) reveal the restored framework compositions, and in each case the way in

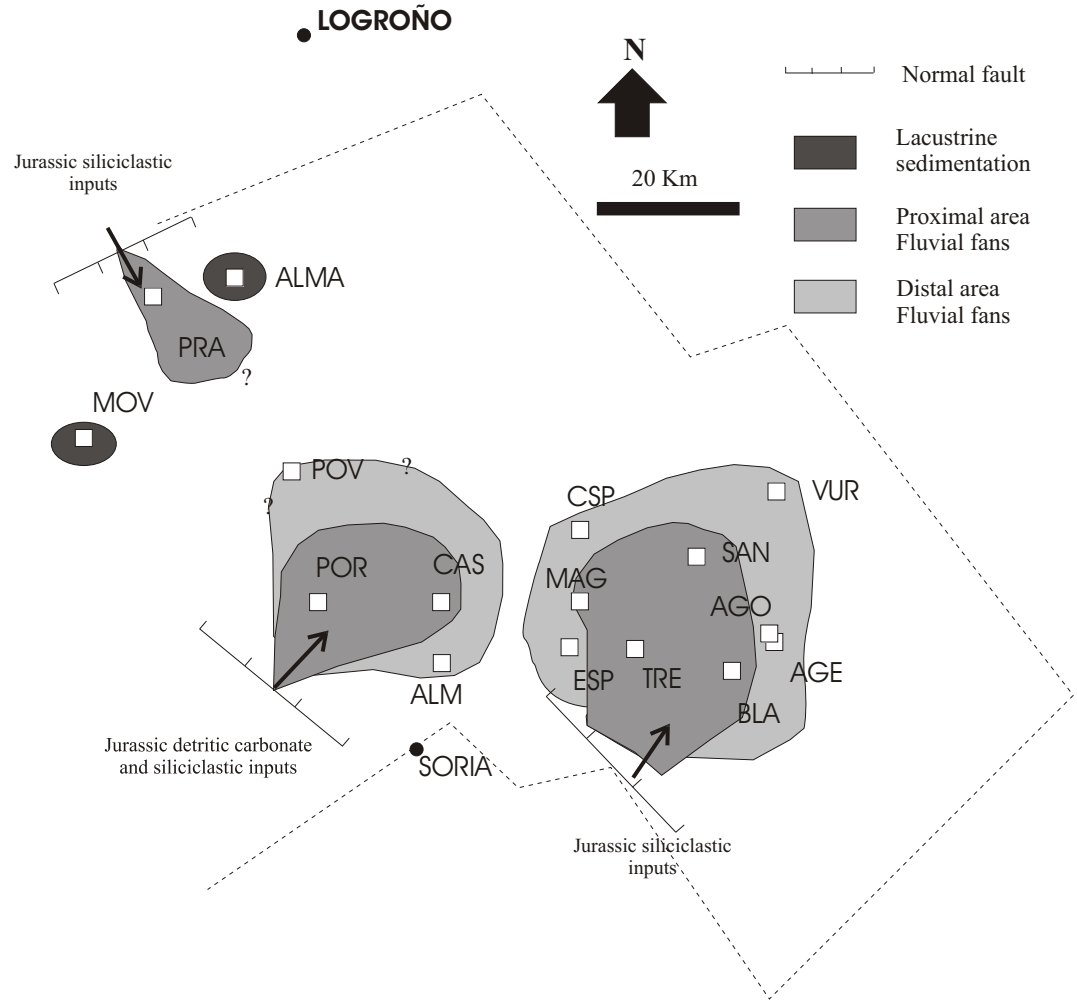

Fig. 3.- Paleogeographic sketch map of the top of the Ágreda Fm. (DS 1). Notice the clear influence of transversal inputs. For names of the stratigraphic sections see caption of Fig. 1.

Fig. 3.- Esquema paleogeográfico para el techo de la Fm. Ágreda (SD 1). Nótese la clara influencia de los aportes transversales. Los nombres de las secciones estratigráficas están indicados en el pie de la Fig. 1.

which composition differs from the original framework is indicated: carbonate replacement of quartz (Cq); kaolinite, kaolinite plus illite, illite or carbonate replacement of K-feldspar (CaoK, Cik, Kill, Ck); illite replacement of albite (Ail); carbonate replacement of plagioclase (Cab); ankerite replacement of carbonate-rock fragments (Afrc). Thirty-two detrital classes were considered and grouped into four categories according to the criteria of Zuffa (1980): Non- Carbonate Extrabasinal (NCE), Carbonate Extrabasinal (CE), Non-Carbonate Intrabasinal (NCI) and Carbonate Intrabasinal (CI) (Tables 1 and 2).

4. Results

4.1. Ágreda Fm

Siliciclastic rocks show a positive correlation between Qmr/Qmo (monocrystalline quartz undulosity <5º vs monocrystaline quartz undulosity >5º) and Qp/Qm (polycrystalline quartz vs monocrystalline quartz) (Fig. 7.A), as well as between P/K (plagioclase vs K-feldspar) and Ms/Qmr (Muscovite/ monocrystalline quartz undulosity <5º) (Fig. 7.B), as manifested in the log-ratio diagrams. The relationship between the indices Qmr/Qmo and Qp/Qm is statistically significant (R^2>0.16, Fig. 7.A). Feldspar (F) in the QmFLt diagram (Fig. 8.A) increases from the northern (1-4%) to the southern part of the study area (12-21%). Samples from the Almajano section (ALM, Fig. 1) possess a different composition in the Ágreda Fm., as compared to the rest of the study area. According, the Ágreda Fm. is represented by two sub-petrofacies named 1A and 1B:

Petrofacies 1A is a quartzolithic petrofacies with a mean composition of $Qm_{84}F_{15}Lt_1$ (Fig. 8.A). It lies near to the Qm-K line on a QmKP diagram, due to the scarcity of plagioclase (Fig. 8.B). Plutonic rock fragments and schist-slate fragments are present, especially towards the south and the top of the formation (AGE, BLA, SAN, ESP, VUR) (Figs. 1 and 8.C). The Qmr/Qmo index is high and tends to increase towards the top of the formation, where some quartz grains with abraded overgrowths are present, and provide evidence of sedimentary recycling (eg: Zuffa, 1987). In addition, limestone-rock fragments are locally abundant to the south in the POR area (Figs. 1 and 8.C). This petrofacies has very low values of the Ms/Qmr index (appendices

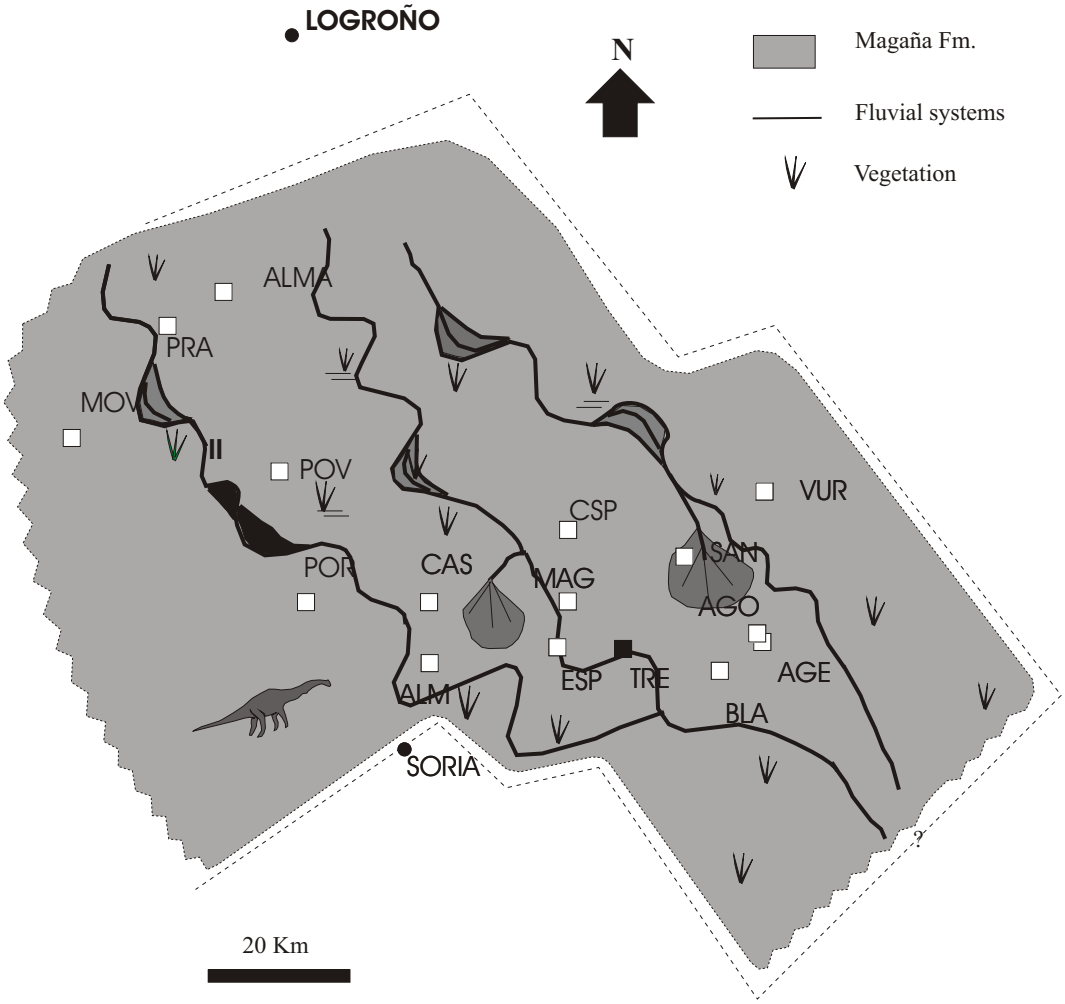

Fig. 4.- Paleogeographic sketch map of the top of the Magaña Fm. (DS 2). Notice the clear influence of axial inputs. For names of the stratigraphic sections see caption of Fig. 1.

Fig. 4.- Esquema paleogeográfico para el techo de la Fm. Magaña (SD 2). Nótese la clara influencia de los aportes axiales. Los nombres de las secciones estratigráficas están indicados en el pie de la Fig. 1.

1-7) and is recognized in all the Ágreda Fm. sections except ALM (Fig. 1).

Petrofacies 1B is a sedimentolithic petrofacies ($Qm_{45}F_1Lt_{54}$, Fig. 8.A), which plots on the Rs pole of a RgRsRm diagram (Fig. 8.C), being very rich in carbonate-rock fragments, mainly micritic carbonate fragments (Fig. 8.D). Extrabasinal carbonate-rock fragments and echinoderm plates were derived from the marine Jurassic cover (Fig. 9.A). Moreover, some layers are rich in intrabasinal carbonate-rock fragments including septarian nodules, derived from the calcretes of the Ágreda Fm. (Fig. 9.B). Plutonic rock fragments appear and become more abundant to the top of the formation (Fig. 9.C). Feldspars and polycrystalline quartz are rare (Fig. 9.A and C). The Qmr/Qmo is high, and some quartz grains display abraded overgrowths. Furthermore, the Ms/Qmr index is very low (appendix 4). This petrofacies is present exclusively in the ALM area (Fig. 1).

4.2. Magaña Fm

The log-ratio diagrams indicate a positive correlation between Qmr/Qmo and Qp/Qm (Fig. 10.A), and between P/K and Ms/Qmr (Fig. 10.B), similar to those of the Ágreda Fm. The relationship between both pairs of indices is statistically significant (R^2>0.08). Sandstones of the Magaña Fm. constitute Petrofacies 2 ($Qm_{77}F_{19}Lt_4$), a quartzofeldspathic petrofacies with variable quartz content (65-91%, Fig. 11.A). The lowest quartz contents are located in the central part of the study area (POV, POR, figs. 1 and 11.A), and locally in the northern (MOV, figs. 1 and 11.A) and southern parts of the study area (MAG, figs. 1 and 11.A). Mean feldspar content is between 6-32%, with the highest values in the northern and central parts of the study area. In general, K-feldspars predominate over plagioclases ($Qm_{80}K_{13}P_{7,}$ Fig. 11.B), being K between 5-26 % and P between 1-11 %.The content in lithic fragments varies between 1-19 %, with the highest values to the northern and central parts of the study area (POR, Fig. 1). There is a clear and local influence of micritic carbonate-rock fragments towards the bottom and top of the formation. Further, plutonic and metamorphic rock fragments (Fig. 9.D) are present. Polycrystalline quartz, usually with tectonic fabric and containing more than three sub-crystal units per grain is common (Fig. 9.E). Muscovite content is generally significant (Fig.

NCE (Non Carbonate Extrabasinal)	**Q**	Qmr	Quartz monocrystalline, undulosity<5º
		Qmo	Quartz monocrystalline, undulosity>5º
		Qm[Q]	Quartz monocrystalline with inherited sintaxial cement
		Qp2-3	Qp2-3 Quartz polycrystalline 2-3
		Qp>3	Quartz polycrystalline >3 subgrains
		Qfrg	Quatrz in plutonic rock fragment.
		Cq	Carbonate replacement on quartz
		Aq	Ankerite replacement on quartz
	K	Ks	K-feldspar, single crystals
		Kfrg	K-feldspar in coarse-grained rock
		KaoK	Kaolinite replacement K-feldspar
		Kaoik	Kaolinite plus illite replacement K-feldspar
		Kil	Illite replacement K-feldspar
		Ck	Carbonate replacement on K-feldspar
		Aq	Ankerite replacement on K-feldspar
	P	Ps	Plagioclase
		Ab	Albite
		Ail	Illite replacement on albite
		Cfrg	Carbonate replacement on plutonic rock fragment
		Cab	Carbonate replacement on plagioclase
	L	Ch	Chert
		Sl	Slate
		Sch	Schist
	M	Ms	Muscovite
		Mfrg	Muscovite in coarse-grained rock
		Ch	Chorite
		OM	Other mica grains
		Tu	Tourmaline
		Op	Opaque
CE (Carbonate Extrabasinal)	**Ls**	Ml	Micritic limestone
		Sc	Sparitic limestone
		Md	Dolomicrite
		Sd	Dolosparite
		Afrc	Ankerite replacement on carbonate rock
		Fo	Fossils
		Ep	Echinoderm plates
NCI (Non-carbonate intrabasinal)		In	Intraclast
CI (Carbonate Intrabasinal)		Ml	Micritic limestone
		Ps	Pseudomatrix

Cm (Cements)	[Ca]	Calcite cement
	[Dol]	Dolomite cement
	[Ank]	Ankerite cement
	[Q]	Quartz cement
	Ank[Q]	Ankerite replacing quartz cement
	C[Q]	Carbonate replacing quartz cement
	[kao]	Kaolinite cement
	Ank[kao]	Ankerite replacing kaolinite cement
	[kao-il]	Kaolinite-illite cement
	[il]	Illite cement
	[Fe]	Fe-oxide cement
	[K]	K-feldspar cement
	[Ab]	Albite cement
	[Ab]	Albite cement

Table 1.- Explanation of counted petrographic grain parameters.
Tabla 1.- Explicación de las clases petrográficas contadas.

TERNARY PLOT	PARAMETERS
NCE-CE-CI	NCE= Qmr+Qmo+Qm[Q]+Qp2-3+Qp>3+Qfrg+ +Cq+Ks+Kfrg+CaoK+Cik+Cil+Ck+Ps+Ab+Ail+ +Cab+Ch+Lm+Ms+Mfrg+Tu+Op CE= Ml+Sc+Md+Sd+Afrc+Fo+Ep CI= In
QFR	Q= Qmr+Qmo+Qm[Q]+Qp2-3+Qp>3+Qfrg+Cq F=Ks+Kfrg+CaoK+Cik+Kil+Ck+Ps+Ab+Ail+Cab R=Qfrp+Kfrg+Mfrg+Lm+CE
QmFLt	Qm= Qmr+Qmo+Qm[Q]+Qp2-3+Qp>3+Qfrg+Cq F=Ks+Kfrg+CaoK+Cik+Kil+Ck+Ps+Ab+Ail+Cab Lt=Ch+Lm+Ml+Sc+Md+Sd+Afrc+Fo+Pe
QmKP	Qm= Qmr+Qmo+Qm[Q]+Qp2-3+Qp>3+Qfrg+Cq K= Ks+Kfrg+CaoK+Cik+Kil+Ck P= Ps+Ab+Ail+Cab
QmrQmoQp	Qmr= Qmr Qmo= Qmo Qp= Qp2-3+ Qp>3
RgRsRm	Rg= Qfrg+Kfrg+Mfrg Rs= CE Rm= Lm
LmLsmLse	Lm= Lm Lsm= Ml+Md+Afrc Lse= Sc+Sd+Fo+Pe

Table 2.- Recalculated parameters used in the ternary plots. See table 1 for abbreviations.
Table 2.- Parámetros recalculados usados en los diagramas ternarios. Ver la tabla 1 para abreviaturas.

9.F), showing an increase in the values of the Ms/Qmr index to the top of the formation (appendices 1-7).

4.3. Sierra de Matute Fm

Neither Qmr/Qmo and Qp/Qm nor K/P and Ms/Qmr present a statistically significant relationship (Fig. 12). Two sub-petrofacies can be defined in this formation: Petrofacies 3A and 3B:

Petrofacies 3A is a quartzofeldspathic petrofacies ($Qm_{78}F_{16}Lt_{6}$), with relative low quartz proportions (Fig. 13.A) reaching their highest value in the southern area of

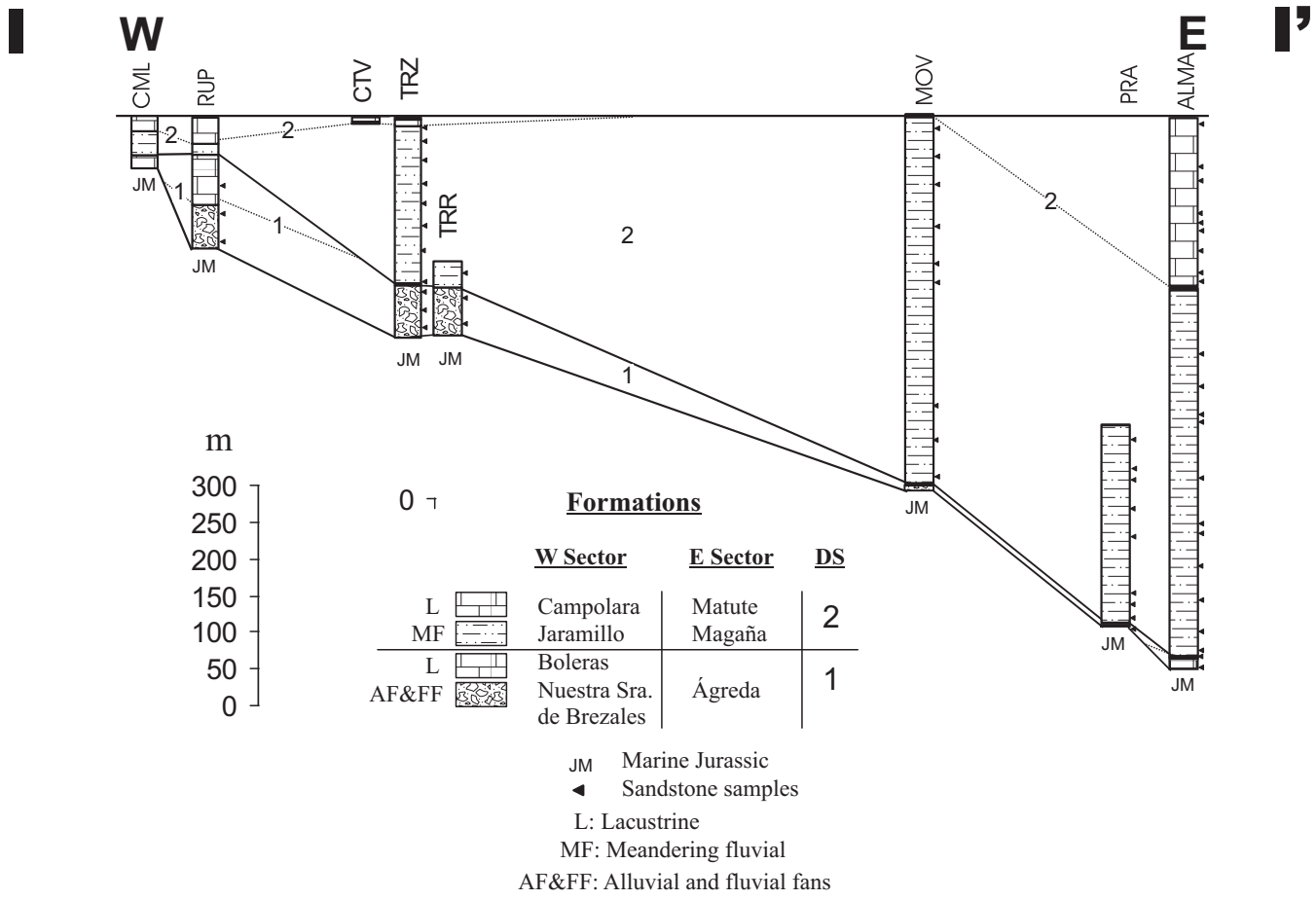

Fig. 5.- Stratigraphic correlation of the northern part of the study area of the Cameros Basin. The orientation is marked in Fig. 1 (I-I'). For names of the stratigraphic section see caption of Fig. 1.

Fig. 5.- Correlación estratigráfica para la parte Norte de la zona de estudio de la Cuenca de Cameros. La orientación está marcada en la Fig. 1 (I-I'). Los nombres de las secciones estratigráficas están indicados en el pie de la Fig. 1.

the studied zone (84%, SAN, Fig. 1). K-feldspar is predominant (9-19%), whereas plagioclase reaches mean proportions of 6-9% ($Qm_{78}K_{13}P_{9,}$ figs. 13.B and 9.H). Rock fragment population is dominated by plutonic and metamorphic rock fragments (Fig. 13.C). There is a local influence of limestone rock fragments in the southern part of the studied zone (CSP, Fig. 1). The Ms/Ms+Qmr index tends to increase towards the top of the formation (appendices 1-7). This petrofacies is recognized in all the stratigraphic sections except ALM (Fig. 1).

Petrofacies 3B is a sedimentolithic petrofacies with a mean composition of $Qm_{76}F_5Lt_{19}$ (Fig. 13.A). Plagioclases are more abundant than K-feldspars ($Qm_{81}K_5P_{14}$, Fig. 13.B). Lithic fragments are relatively abundant (Fig. 13.C), showing a clear predominance of sparitic rock fragments and inherited echinoderm plates (Figs. 13.D and 9.I). Scarce schist-slate fragments occur ($Lm_1Lsm_{45}Lse_{54}$, Fig. 11.D). This Petrofacies is only present in the southern part of the study area near the ALM locality (Fig. 1).

6. Discussion

6.1. Source areas and paleodrainage implications in the western Cameros Basin

The changes observed in the petrofacies examined in this study (Fig. 14) indicate variations in source areas during the sedimentation of the Tera Group.

Petrofacies 1A, observed in the Ágreda Fm. (DS 1), lies near the Qm-F side of the QmFLt diagram (Figs. 8.A and 14.A) and is rich in K-feldspars (Figs. 8.B and 14.B), indicating derivation from plutonic source areas. In spite of the scarcity of plutonic rock fragments in the sandstone framework (<1.4 %), the presence of these grains is very significant, because they tend to form sands composed by monomineral grains (eg: Zuffa, 1985, Palomares and Arribas, 1993). Subordinate contributions from metamorphic source areas are also indicated (Figs. 8.C and 14.C). Local erosion of limestone source areas is observed at the southern part of the study area (POR, figs.

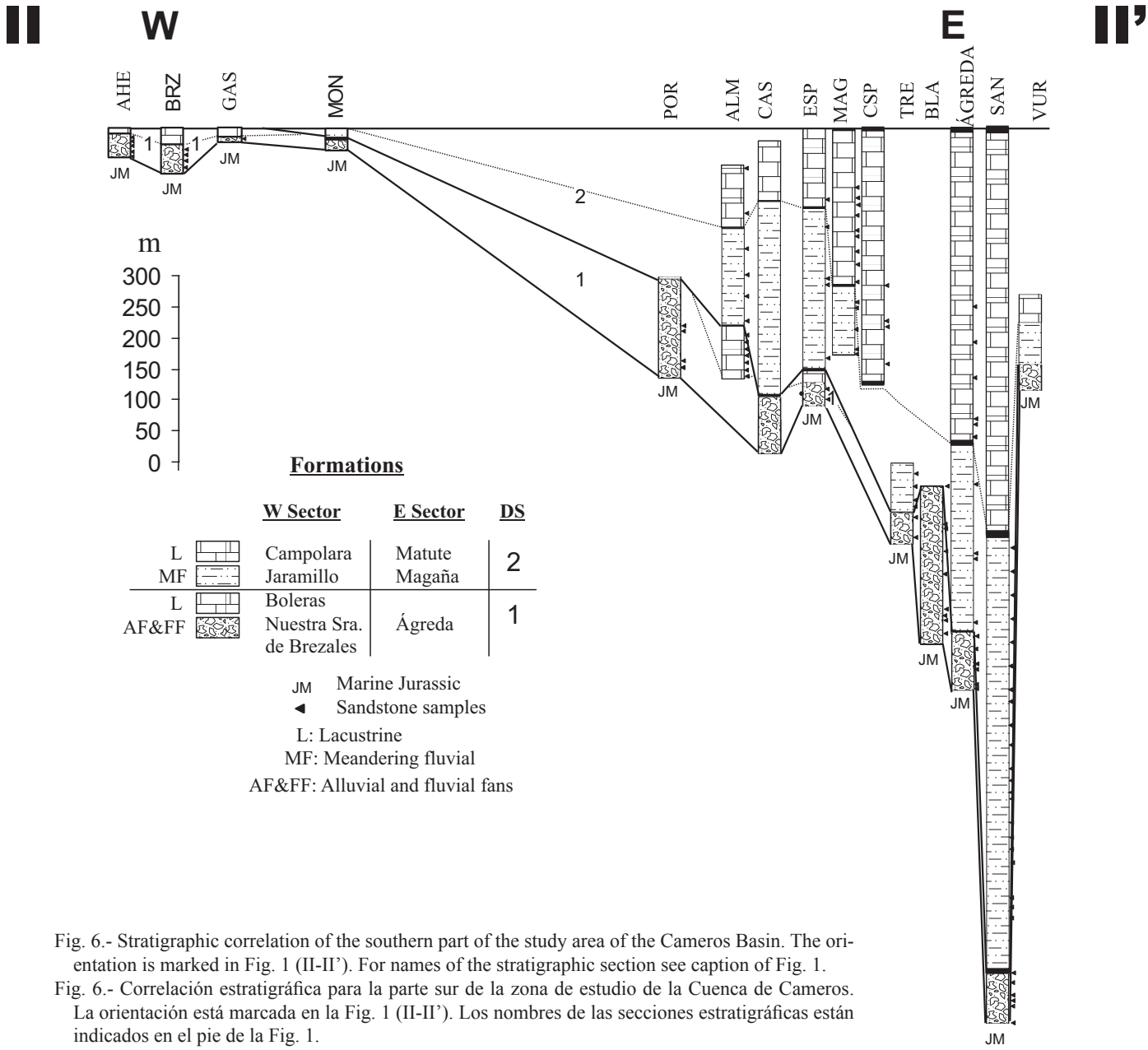

Fig. 6.- Stratigraphic correlation of the southern part of the study area of the Cameros Basin. The orientation is marked in Fig. 1 (II-II'). For names of the stratigraphic section see caption of Fig. 1.

Fig. 6.- Correlación estratigráfica para la parte sur de la zona de estudio de la Cuenca de Cameros. La orientación está marcada en la Fig. 1 (II-II'). Los nombres de las secciones estratigráficas están indicados en el pie de la Fig. 1.

1, 8.C and D, 14.C and D). The inferred principal source areas of Petrofacies 1A are nearby granites of the Central Iberian Zone of the Iberian Massif (CIZ, Fig. 15). The more important plutonic input towards the southern part of the study area (AGE, BLA, SAN, ESP, VUR, Fig. 1) is probably related to the paleogeography of this area, which may constitute a different fluvial-fan system (Fig. 3), which could present a higher erosion level of the CIZ. The main bedrock lithologies in the CIZ are Hercynian granites, granodiorites, and gneisses, with minor exposure of low-grade metamorphic rocks (Villaseca *et al.*, 1993; Martínez-Catalán, 2004).

In petrofacies 1B most of the micritic carbonate fragments are intrabasinal, and were probably derived from coeval calcretes of the Ágreda Fm. Sparitic rock fragments in Petrofacies 1 were supplied by the marine Jurassic sedimentary substratum. The high Qmr/Qm index and the presence of quartz with abraded syntaxial overgrowths suggest that both Petrofacies 1A and 1B records the erosion of pre-rift Mesozoic siliciclastic units.

A provenance from metamorphic and granite terranes can be deduced for Petrofacies 2. Despite the low percentage of slate-schist fragments (<2%), the presence of these fragments is highly significant. Several studies of modern sediments (Palomares and Arribas, 1993; Arribas and Tortosa, 2003; Le Pera and Arribas, 2004) have demonstrated that sandstone composition does not allow direct quantitative estimations of the lithologies at the

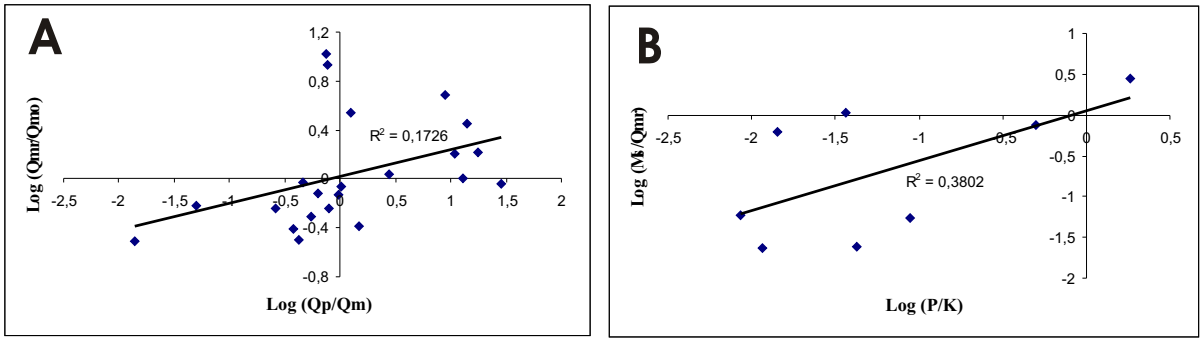

Fig. 7.- Log-ratio diagrams of (A) Qmr/Qmo vs Qp/Qm and (B) Ms/Qmr vs P/K for the Ágreda Fm. (DS 1).
Fig. 7.- Diagramas de los logaritmos de las relaciones (A) Qmr/Qmo vs Qp/Qm y (B) Ms/Qmr vs P/K para la Fm. Ágreda (SD 1).

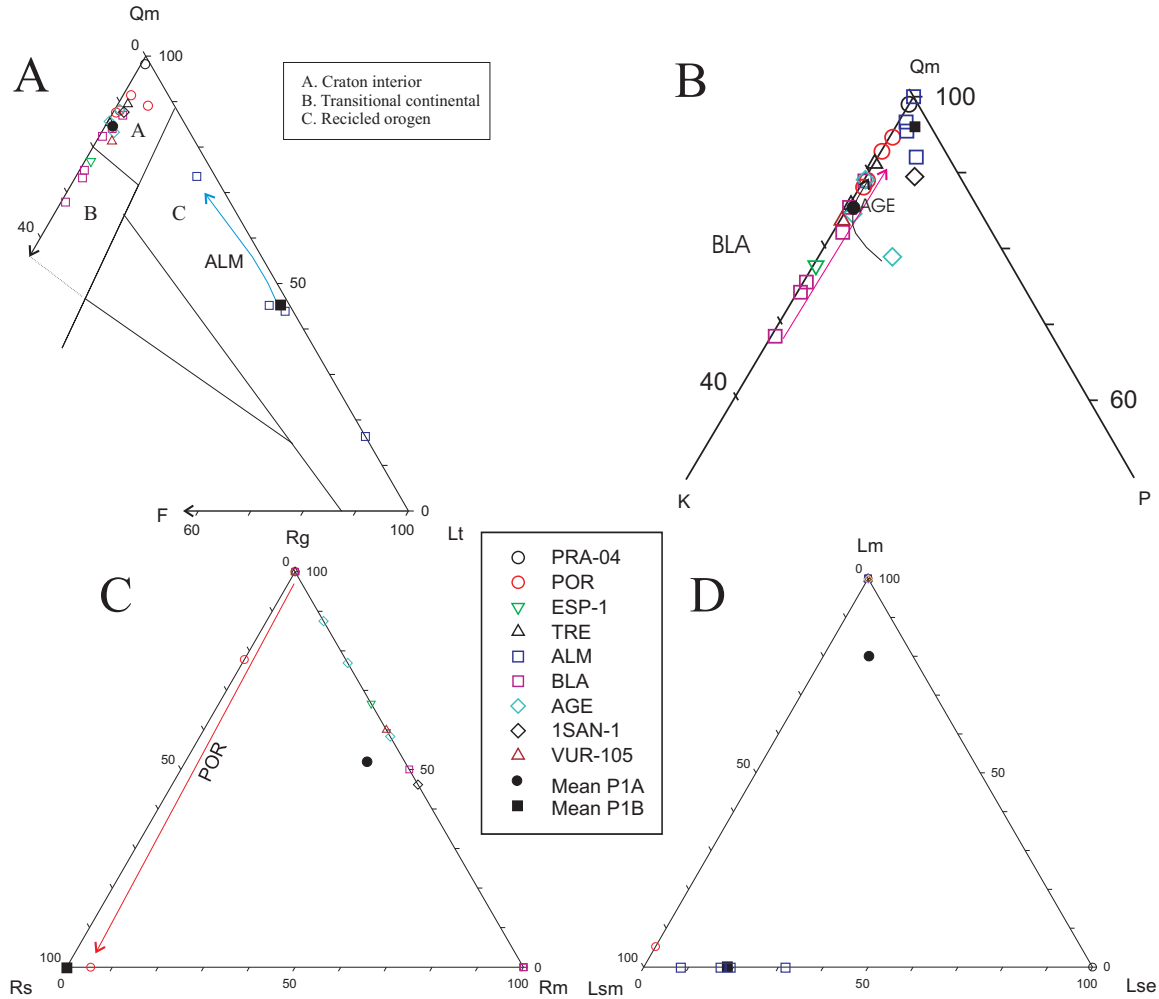

Fig. 8.- Ternary plots describing sandstone composition of the Ágreda Fm. (DS 1). See Table 2 for recalculated parameters and appendices 1-7 for numerical values. The ternary diagrams were prepared according to the criteria of several authors: A.- Dickinson *et al.*, 1983 (QmFLt); B.- Dickinson, 1985 (QmKP); C.- Arribas *et al.*, 1990 and Critelli and Le Pera, 1994 (RgRsRm); D.- Arribas *et al.*, 2002 and 2003 (LmLsmLse). For names of the stratigraphic sections see caption of Fig. 1.
Fig. 8.- Diagramas ternarios para la composición de las areniscas de la Fm. Ágreda (SD 1). Ver la Tabla 2 para los parámetros recalculados y los apéndices 1-7 para los valores numéricos. Los diagramas ternarios se han calculado de acuerdo con los criterios de varios autores: A.- Dickinson *et al.*, 1983 (QmFLt); B.- Dickinson, 1985 (QmKP); C.- Arribas *et al.*, 1990 and Critelli and Le Pera, 1994 (RgRsRm); D.- Arribas *et al.*, 2002 and 2003 (LmLsmLse). Los nombres de las secciones estratigráficas están indicados en el pie de la Fig. 1.

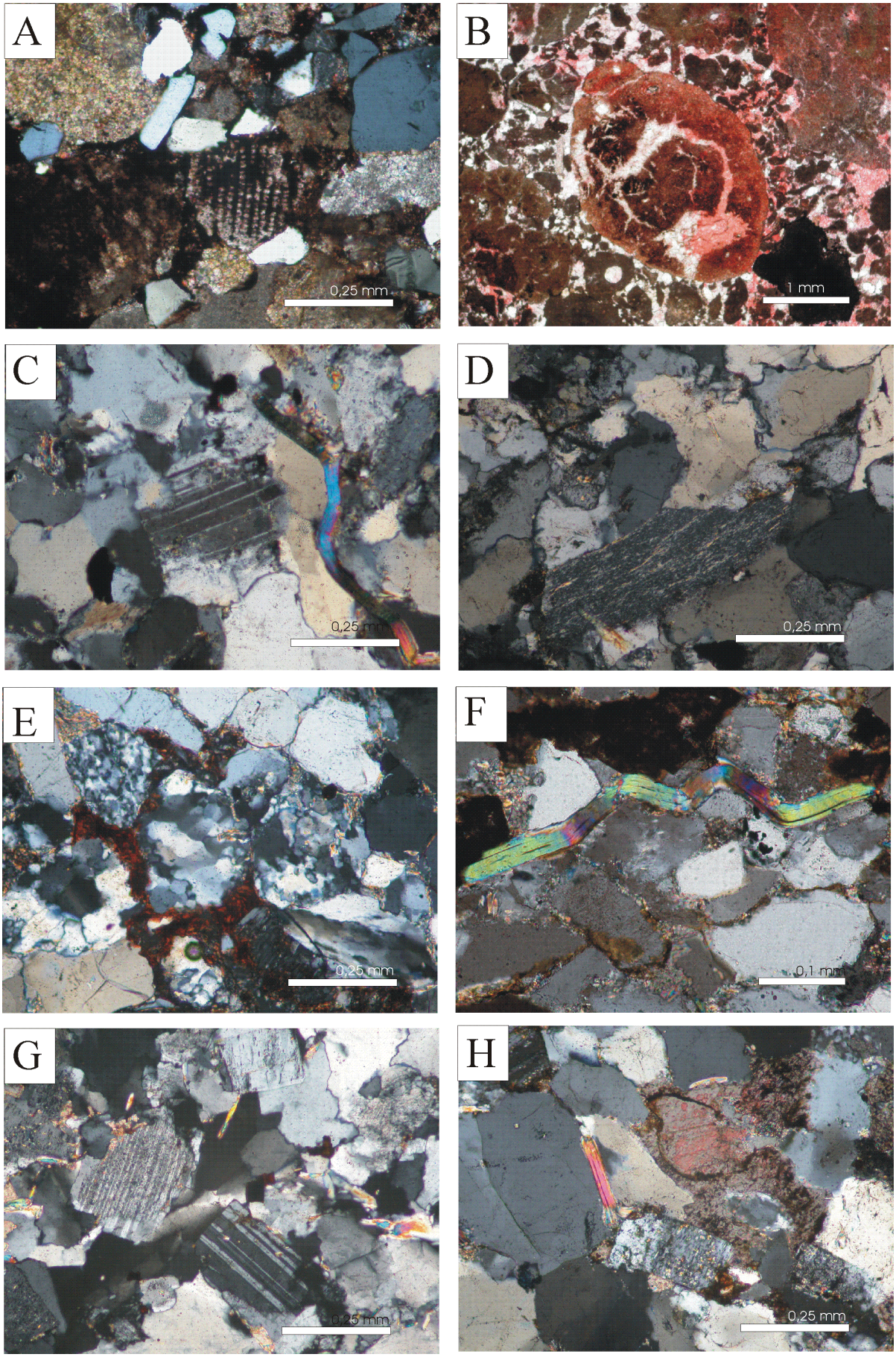
A
0,25 mm
B
1 mm
C
0,25 mm
D
0,25 mm
E
0,25 mm
F
0,1 mm
G
0,25 mm
H
0,25 mm

source, owing to the different capacities of rocks to generate sands (eg: Ingersoll *et al.*, 1984, Zuffa, 1985, Palomares and Arribas, 1993). Indeed, slates and schist have a very low "Sand Generation Index" (Palomares and Arribas, 1993) and are often underrepresented in the sands derived from them, because of their low rock-fragment content in the medium-sand sized detritus. Slate-schist fragments are therefore considered significant despite their scarcity. The inferred source areas for Petrofacies 2 are low-grade to medium-grade metamorphic terranes, which probably correspond to the West Asturian Leonese Zone of the Iberian Massif (WALZ, Fig. 15), as well as plutonic terranes of the CIZ, indicated by feldspar content and presence of Rg fragments. The WALZ consists mainly of a thick lower Paleozoic sequence of slates and quartzites of greenschist facies and minor contents of amphibolite facies (Julivert, 1983, Marcos *et al.*, 2004).

There are important differences between Petrofacies 2 and Petrofacies 1. The proportion of feldspar grains increases from Petrofacies 1 to Petrofacies 2 (Fig. 14.A). In addition, plagioclase is present in Petrofacies 2 (Figs. 11.B and 14.B), whereas in Petrofacies 1A plagioclase is absent or or very scarce (Figs. 8.B and 14.B). This evidence probably indicates a change in the type of eroded plutonic rocks of the CIZ from Petrofacies 1 to Petrofacies 2. Plutonic source areas for Petrofacies 2 could have had a mixed composition (potassium and calcium-sodium) to generate both K-feldspar and plagioclase, whereas plutonic source areas of Petrofacies 1 were probably predominantly of potassium-rich composition. This change could indicate a difference from the paleogeographic location of the plutonic source areas in the CIZ or a different level of erosion reached after the sedimentation of the DS 1. In addition, there is a clear increase in the Ms/Qmr index between both petrofacies and to the top of Petrofacies 2 (appendices 1 to 7), which could be related either to the possible change of the plutonic source area composition or to the increase in the plutonic and metamorphic influence in Petrofacies 2. Furthermore, the Qp/Qt index increases from Petrofacies 1 to Petrofacies 2 due to the higher influence of metamorphic source rocks, which is also demonstrated by the higher proportions of metamorphic rock-fragments in the Petrofacies 2 compared to the Petrofacies 1 (Fig. 14.C).

These differences recorded between Petrofacies 1A and 2 are clearly related to the sedimentology of both depositional sequences. In this sense, the provenance of the conglomerates and sandstones of the Ágreda Fm. (Petrofacies 1A, DS 1) is controlled by the relationship between tectonics and sedimentation of fluvial-fans implying transversal inputs to the basin (Figs. 3 and 16). Local source areas (mainly composed of marine Jurassic limestones and siliciclastic Mesozoic units) were clear important, especially in the Petrofacies 1B. However, the provenance for the detritus in the meandering fluvial systems of the Magaña Fm. (Petrofacies 2, lower part of DS 2) is related to different source areas because these systems were dominated by axial dispersal in the basin (Figs. 4 and 16), which resulted a higher contribution from the metamorphic source areas (WALZ) and the erosion of different plutonic source rocks with mixed composition (CIZ). The higher organization of the meandering fluvial systems of the DS 2 suggests longer distance transport, implying different source areas. In this sense, intrabasinal carbonates are more common in petrofacies representing the fluvial-fans (1A and B) than in the petrofacies related to meandering fluvial systems (2), due to the abundance of calcretes in the distal areas of the fluvial-fans.

Petrofacies 3A manifests a clear influence of metamorphic and plutonic source areas as shown by high values of the Ms/Qmr and Qp/Qt, and low values of the Qmr/Qm. Ms/Qmr and Qp/Qt tend to increase towards the top of

Fig. 9.- (previous page) Photomicrographs of the detrital components and diagenetic features of the Tera Group sandstones. Crossed nichols. A.- Inherited echinoderm plate (ALM, Petrofacies 1B, Ágreda Fm.). B.- Septarian nodule of a calcrete (Petrofacies 1B, Ágreda Fm.). C.- Plutonic rock-fragment (ALM, Petrofacies 1B, top of the Ágreda Fm.). D.- Slate fragment (ESP, Petrofacies 2, Magaña Fm.). E.- Polycrystalline quartz grains with more than 3 sub-crystal units, showing tectonic fabric with the exception of the central grain (ESP, Petrofacies 2, Magaña Fm.). F.- Medium-grained arkose from the Magaña Fm. Notice the presence of K-feldspars (indicated with K labels). Muscovite exhibits features of mechanical compaction (MOV, Petrofacies 2, Magaña Fm.). G.- Medium-grained subarkose from the Sierra de Matute Fm. Notice the abundance of polysynthetic plagioclase with syntaxial overgrowths. The framework exhibits dense packing generated by compaction (AGE, Petrofacies 3A). H.- Subarkose from the Sierra de Matute Fm. presenting a sparitic rock-fragment. Note the presence of muscovite and albite (ALM, Petrofacies 3B).

Fig. 9.- (página anterior) Fotografías de microscopio de los componentes detríticos y los rasgos diagenéticos de las areniscas del Grupo Tera. Nícoles cruzados. A.- Placa de equinodermo heredada (ALM, Petrofacies 1B, Fm. Ágreda). B.- Nódulo septarizado de una calcreta (Petrofacies 1B, Fm. Ágreda). C.- Fragmento de roca plutónica (ALM, Petrofacies 1B, techo de la Fm. Ágreda). D.- Fragmento de pizarra (ESP, Petrofacies 2, Fm. Magaña). E.- Cuarzos policristalinos con más de tres unidades cristalinas, mostrando fábrica tectónica excepto el grano central (ESP, Petrofacies 2, Fm. Magaña). F.- Arcosa de grano medio de la Fm. Magaña. Nótese la presencia de feldespatos K (marcados con K). La moscovita muestra rasgos de compactación mecánica (MOV, Petrofacies 2, Fm. Magaña). G.- Subarcosa de grano medio de la Fm. Sierra de Matute. Nótese la abundancia de plagioclasa polisintética con cementos sintaxiales. El esqueleto muestra un empaquetado denso generado por compactación (AGE, Petrofacies 3A). H.- Subarcosa de la Fm. Sierra de Matute que presenta un fragmento de roca esparítico. Nótese la presencia de moscovita y albita (ALM, Petrofacies 3B).

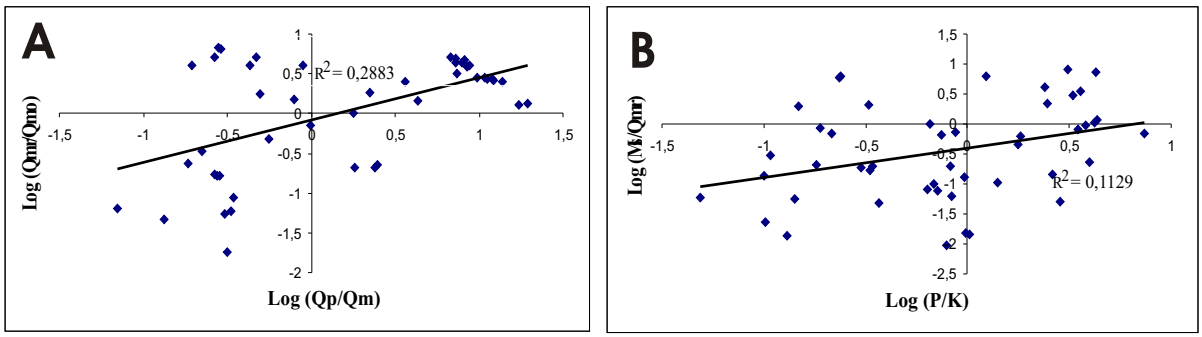

Fig. 10.- Log-ratio diagrams of (A) Qmr/Qmo *vs* Qp/Qm and (B) Ms/Qmr *vs* P/K for the Magaña Fm. (DS 2).
Fig. 10.- Diagramas de los logaritmos de las relaciones (A) Qmr/Qmo vs Qp/Qm y (B) Ms/Qmr vs P/K para la Fm. Magaña (SD 2).

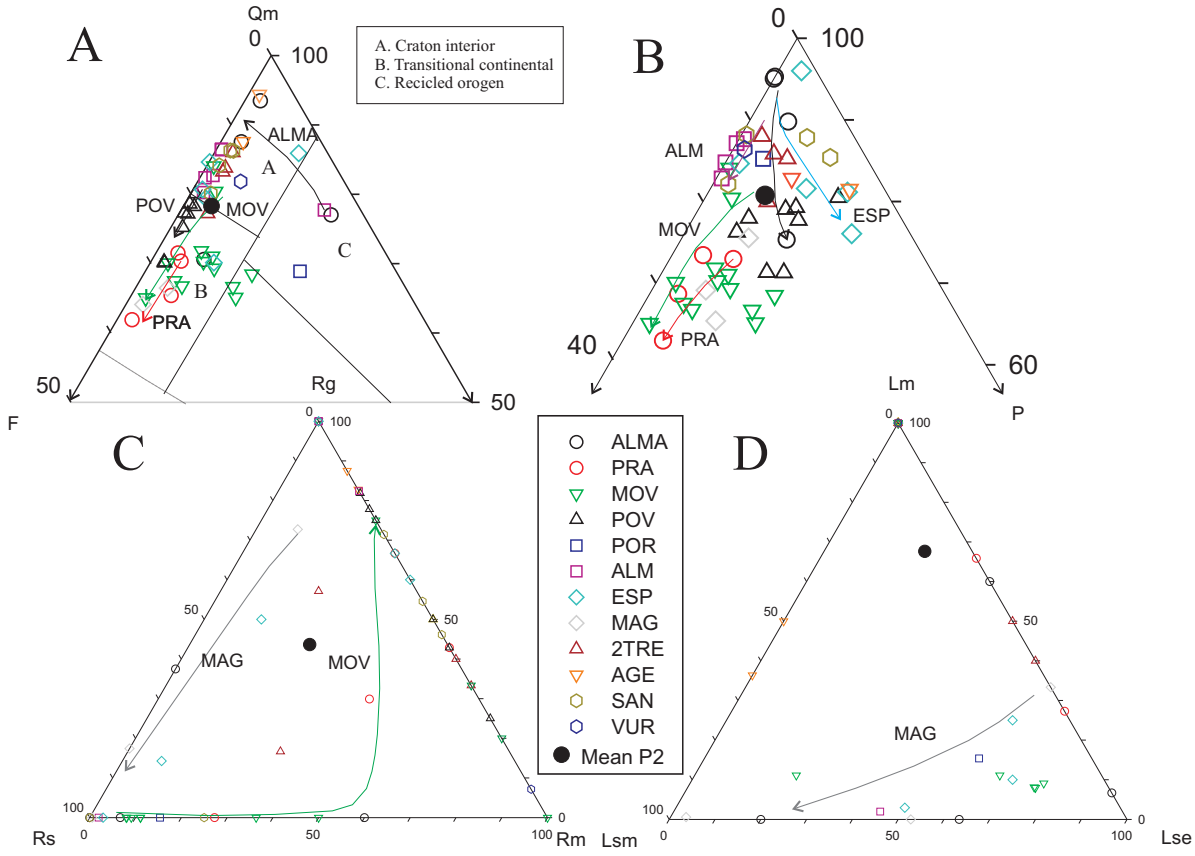

Fig. 11.- Ternary plots describing sandstone composition of the Magaña Fm. (DS 2). See Table 2 for recalculated parameters and appendices 1-7 for numerical values. For names of the stratigraphic section see caption of Fig. 1.
Fig. 11.- Diagramas ternarios para la composición de las areniscas de la Fm. Magaña (SD 2). Ver la Tabla 2 para los parámetros recalculados y los apéndices 1-7 para los valores numéricos. Los nombres de las secciones estratigráficas están indicados en el pie de la Fig. 1.

the formation, whereas Qmr/Qm tends to decrease. Petrofacies 3A presents equivalent plutonic source areas than Petrofacies 2, but with mixed potassium and calcium-sodium composition of feldspar framework grains (Fig. 14.B). Petrofacies 3A presents higher quartz and lower feldspar proportion compared to Petrofacies 2 in relation mainly to the decrease of K-feldspar (Figs. 14.A.B). The amount of plagioclase is higher to the south of the Sierra de Matute Fm. (Fig. 13.B).

Plutonic and metamorphic source rocks constituted the main influence for both sub-petrofacies (3A and 3B), displaying more important local inputs from the Jurassic marine substrate in the Petrofacies 3B (Fig. 14.C). The abundance of sparitic rock-fragments (Fig. 14.D) and the

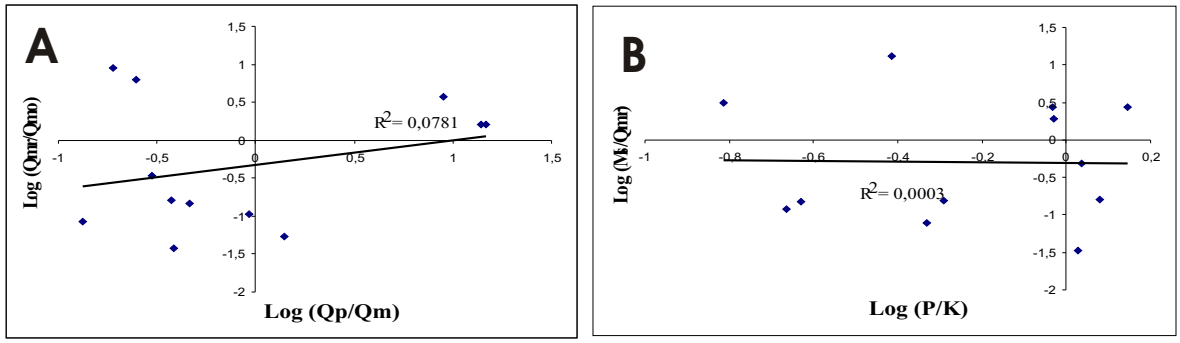

Fig. 12.- Log-ratio diagrams of (A) Qmr/Qmo *vs* Qp/Qm and (B) Ms/Qmr *vs* P/K for the Sierra de Matute Fm. (DS 2).
Fig. 12.- Diagramas de los logaritmos de las relaciones (A) Qmr/Qmo vs Qp/Qm y (B) Ms/Qmr vs P/K para la Fm. Sierra de Matute (SD 2).

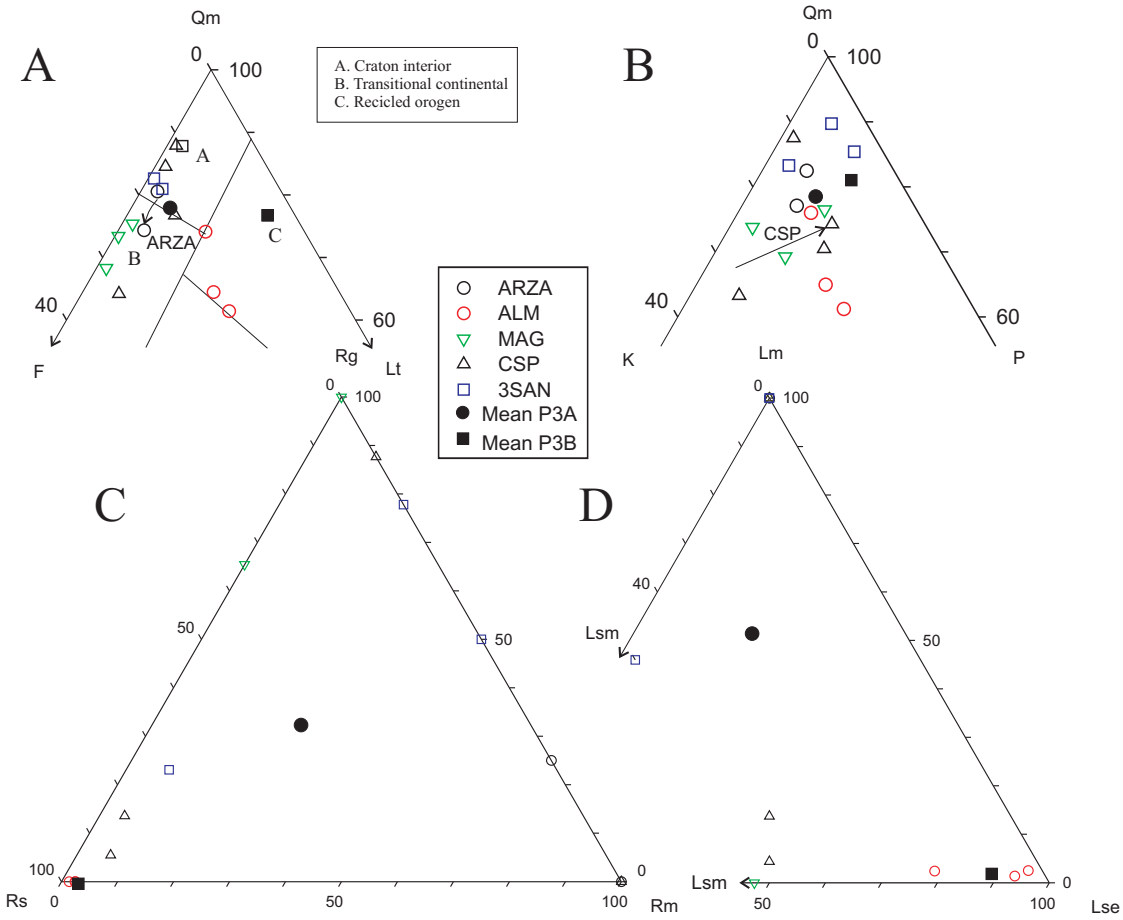

Fig. 13.- Ternary plots describing sandstone composition of the Sierra de Matute Fm. (DS 2). See Table 2 for recalculated parameters and appendices 1-7 for numerical values. For names of the stratigraphic section see caption of Fig. 1.
Fig. 13.- Diagramas ternarios para la composición de las areniscas de la Fm. Sierra de Matute (SD 2). Ver la Tabla 2 para los parámetros recalculados y los apéndices 1-7 para los valores numéricos. Los nombres de las secciones estratigráficas están indicados en el pie de la Fig. 1.

presence of inherited echinoderm plates in Petrofacies 3B indicate erosion of the Jurassic marine substrate, as in Petrofacies 1B. Furthermore, the increase in the Qmr/Qm index from Petrofacies 2 to Petrofacies 3B could indicate a higher influx of sedimentary siliciclastic source areas if compare to the top of Petrofacies 2. The erosion of the Jurassic marine source areas in Petrofacies 3B has been interpreted as the result of a change in the location of rift-bounding faults (back faulting process) in this area, related to the evolution of the rift system (González-Acebrón *et al.*, 2007). Finally, in Petrofacies 3B, a secondary influence of metamorphic source areas is recorded by the scarce schist-slate fragments and polycrystalline quartz with tectonic fabric.

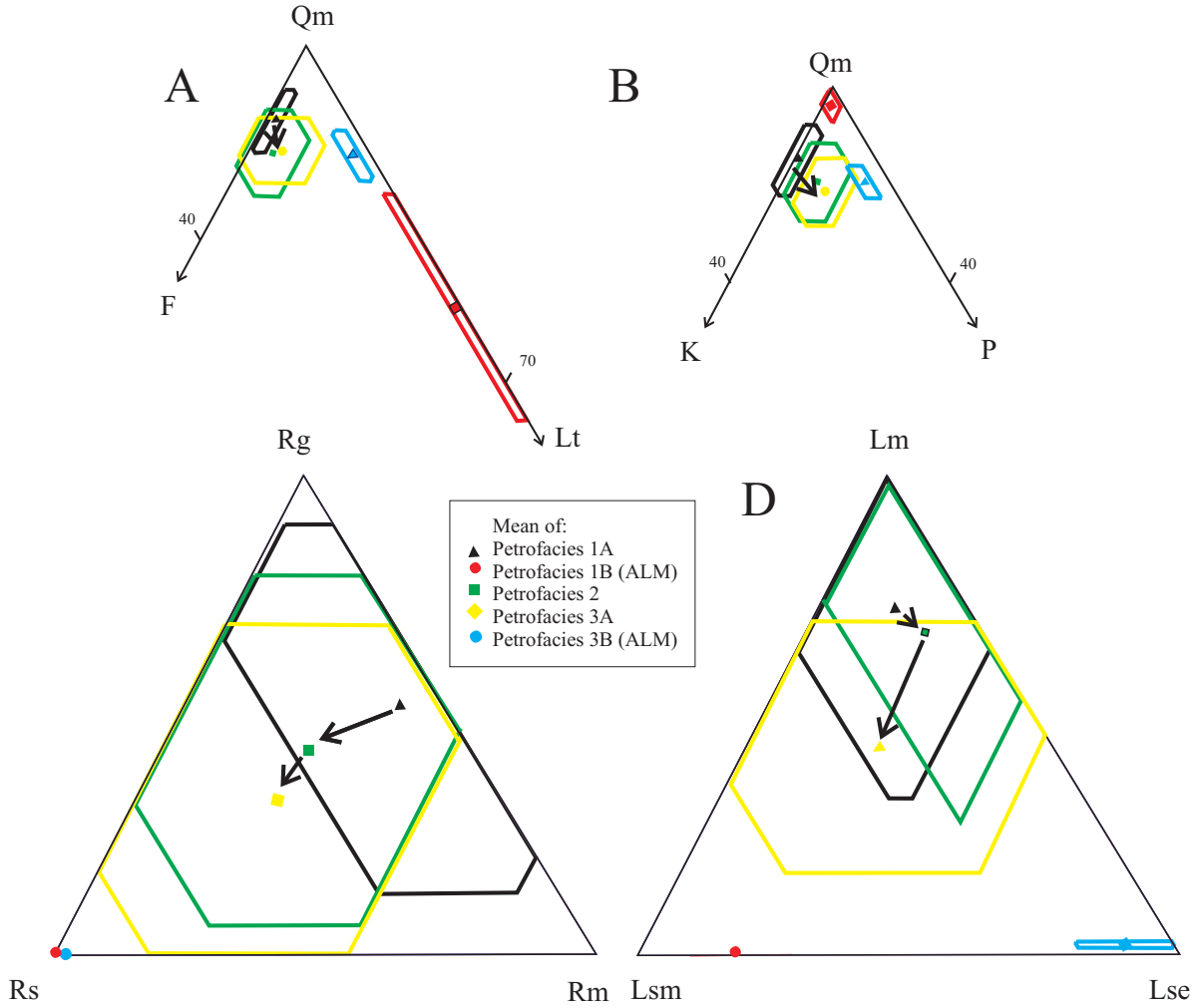

Fig. 14.- Ternary plots resuming sandstone composition of the Tera Group. Each petrofacies is marked by its arithmetic average and a hexagon for its standard deviations. The arrows indicate the evolution from Petrofacies 1A to Petrofacies 2 and finally to Petrofacies 3A. See Table 2 for recalculated parameters and appendices 1-7 for numerical values.

Fig. 14.- Diagramas ternarios que resumen la evolución de la composición de las areniscas del Grupo Tera. Cada petrofacies está marcada por su media aritmética y un hexágono que marca sus desviaciones estándar. Las flechas indican la evolución desde la Petrofacies 1A a la Petrofacies 2 y finalmente a la Petrofacies 3A. Ver la Tabla 2 para los parámetros recalculados y los apéndices 1-7 para los valores numéricos.

6.2. Implications for the Cameros Basin and sandstone provenance in rift systems.

Petrofacies 1 corresponds to the undissected-transitional stage of the non-volcanic rifted margin model of Garzanti *et al.* (2001, 2003). This type of provenance has been recognized in modern sands of the Red Sea and Gulf of Aden (Yemen). Petrofacies 1 shows many features of this stage: it plots in the compositional area for the undissected-transitional stage of the QmFLt ternary plot and shows sedimentary detritus, including recycled monocrystalline quartz and carbonate grains. We further propose that the undissected-transitional stage has high log-ratio values of Qmr/Qmo, and low log-ratio values of Qp/Qm, P/K and Ms/Qmr (Fig. 16).

The increase of feldspar content recorded from Petrofacies 1 to Petrofacies 2 and 3 probably indicates an increase in basement erosion. This compositional trend indicates a change from undissected-transitional to transitional-dissected signatures (Garzanti *et al.*, 2001, 2003). During the transitional stage, sands are derived from sedimentary successions and underlying basement rocks in varying proportions, as a function of the erosion level and type of rocks exposed, whereas during the dissected stage detritus from the basement rocks is dominant (Garzanti *et al.*, 2001, 2003). Our findings indicate that during the transitional-dissected stage Qmr/Qmo decreases, whereas Qp/Qm and Ms/Qmr normally tend to increase towards the top (Fig. 16). The tendencies of the P/K index are locally variable depending on the feldspar

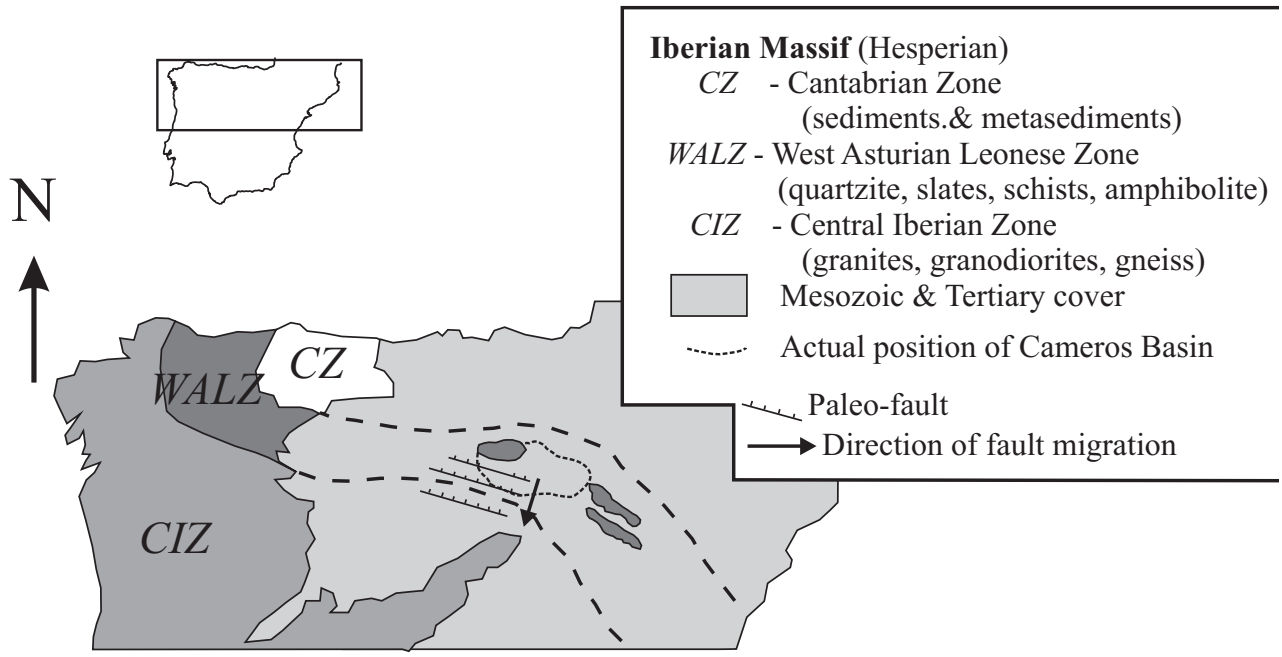

Fig. 15.- Location of the West Asturian Leonese Zone (WALZ) and the Central Iberian Zone (CIZ) in the scheme of Julivert *et al.* (1972) for the Iberian (Hesperian) Massif. The arrow indicates direction of fault migration during the tectonic development of the basin, from the Late Jurassic to Middle Albian (modified from Arribas *et al.*, 2003). The two bold dashed lines indicate the borders of the WALZ below the Cenozoic cover.

Fig. 15.- Localización de la Zona Asturoccidental Leonesa (WALZ) y de la Zona Centroibérica (CIZ) en el esquema de Julivert *et al.* (1972) para el macizo Ibérico (Hespérico). La flecha indica la dirección de migración de fallas durante el desarrollo tectónico de la cuenca, desde el Jurásico tardío al Albiense medio (modificada de Arribas *et al.*, 2003). Las dos líneas discontinuas indican el límite de la WALZ bajo la cobertera cenozoica.

composition of the plutonic or metamorphic source areas, but the P/K ratios are higher than in the undissected-transitional stage. We infer that these are general trends for non-volcanic rift basins with mainly source plutonic and/or metamorphic source areas.

Petrofacies 3B corresponds to the undissected-transitional stage of Garzanti *et al.* (2001, 2003), due to the increasing relevance of sedimentary sources and the reactivation of this part of the basin by a back faulting process (González-Acebrón *et al.*, 2007).

The provenance evolution of the western Tera Group is equivalent that of the eastern Tera Group, studied by Arribas *et al.* (2003). Petrofacies A of those authors is equivalent to Petrofacies 1B of this study. Both have similar QmFLt compositions (A: $Qm_{85}F_2Lt_{13;}$ 1B: $Qm_{45}F_{1-2}Lt_{53-54}$), as well as important amounts of Jurassic marine rock fragments. Both petrofacies 1A (this study) and A (Arribas *et al.*, 2003) represent higher degrees of rift-margin erosion than Petrofacies 1B (this work), because both 1A and A imply the erosion of the exhumed metamorphic basement.

Petrofacies 2 of this study is equivalent to Petrofacies B (Arribas *et al.*, 2003) of the western Cameros Basin. The main difference between these petrofacies is the presence of plutonic rock fragments in Petrofacies 2, which are absent from Petrofacies B. Thus, deeper erosion of the basement was recorded in sediments of Tithonian age from the eastern sector of the basin.

Our study shows that the use of RgRsRm and LmLs-mLse diagrams and log-ratio diagrams of Qmr/Qmo, Qp/Qm, P/K and Ms/Qmr indices are important for a comprehensive provenance analysis in rifted basins. The Qmr/Qmo index correlates positively with the Qp/Qm index, which is statistically significant only if there are enough studied samples.

7. Conclusions

The provenance of the fluvial-fan sandstones deposited during the beginning of the rifting (undissected rift shoulder and transitional stage) within the Cameros basin is controlled by the composition of local source areas, as well as by the relationship between tectonics and sedimentation of these fluvial-fans. On the contrary, the provenance in the fluvial systems deposited during more advanced stages of the rifting (dissected rift shoulder) is related to different source areas and changes due to the progressive erosion of the basement rocks. This provenance evolution is due to the higher influence of transverse dispersal during the fluvial-fan stage to more important axial inputs

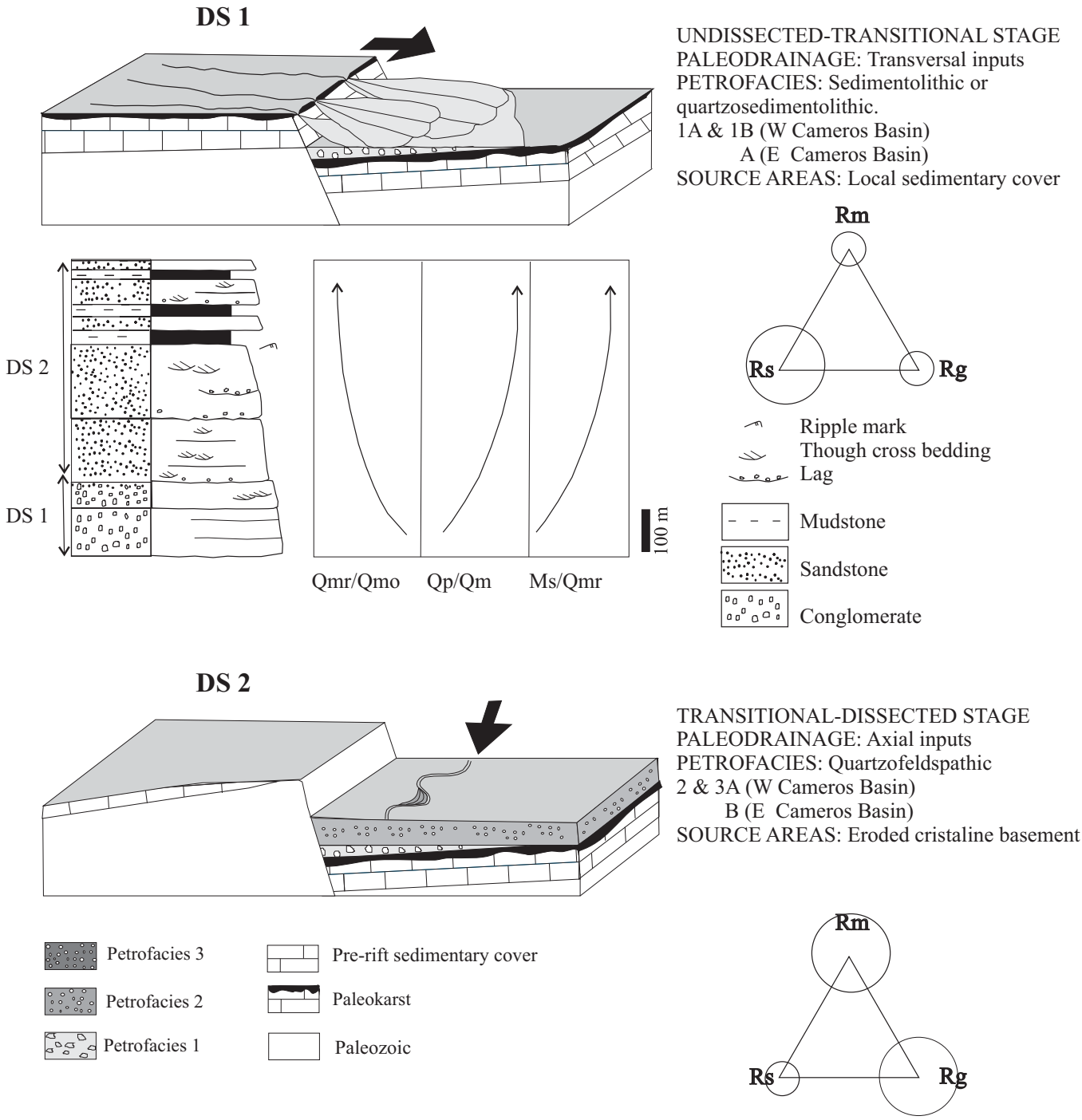

Fig. 16.- Summary of the tectonic evolution and its relation to the sedimentation of DS 1 and 2 during the rift, showing the petrographic characteristics and main indices, as well as the RgRsRm ternary plot. The index diagrams only show tendencies, and the circles on the ternary plots represent the relative abundance of the different rock fragments. Petrofacies of the eastern Cameros Basin are referred to Arribas *et al.*, 2003.

Fig. 16.- Resumen de la evolución tectónica y su relación con la sedimentación de las SD 1 y 2 durante el rift, mostrando las características petrográficas y los principales índices, así como el diagrama RgRsRm. Los diagramas de los índices sólo muestran tendencias, y los círculos en los diagramas triangulares señalan las abundancias relativas entre los distintos fragmentos de roca. Las petrofacies del sector occidental de la Cuenca de Cameros Basin se refieren al trabajo de Arribas *et al.*, 2003.

during the fluvial stage. Our study demonstrates how ancient drainage patterns in rift basins can be characterized using sandstone provenance. Changes in major drainage reorganization driven by a change in rift style imply different degrees of recycling of the pre-rift sedimentary cover and changes in the level of unroofing and erosion of the basement.

The presence of plutonic rock fragments in the eastern Cameros Basin, which have not been recognized in the western Cameros Basin, indicates a deeper level of erosion of the basement in the eastern sector, implying differences in the rift evolution of both parts of the basin.

Finally, the Tera Group represents the start of a provenance cycle in a non-volcanic rifted basin, evolving from petrofacies with high recycling grade (quartzosedimentolithic or quartzolithic) to petrofacies with higher influence of plutonic and metamorphic source areas (quartzofeldspathic petrofacies).

Acknowledgements

Funding for this research was provided by the Spanish DIGICYT projects BTE 2001-026, CGL 2005-07445-C03-02/BTE and CGL 2008-01648/BTE. The authors would like to thank Herrero, G., Moral, B. and Barajas, M.A. for their technical support. This manuscript benefits the useful comments of Emilia Le Pera and Timothy F. Lawton.

Appendices. Supplementary data

Supplementary data associated with this article can be found, in the online version, at www.ucm.es/JIG:

Appendices 1 and 2: Modal petrographic analyses of the north area of the eastern Cameros Basin sandstones. See table 1 for petrographic parameters and Fig. 1 for the location of the stratigraphic sections.

Appendix 3: Modal petrographic analysis of sandstones from the central area of the eastern Cameros Basin. See table 1 for petrographic classes and Fig. 1 for the position of the stratigraphic sections.

Appendices 4, 5, 6 and 7: Modal petrographic analyses of the south area of the eastern Cameros Basin. See table 1 for petrographic classes and Fig. 1 for the position of the stratigraphic sections.

References

Arribas, J., Tortosa, A. (2003): Detrital modes in sedimenticlastic sand from low-order streams in the Iberian Range, Spain: The potential for sand generation by different sedimentary rocks. *Sedimentary Geology*, 159: 275-303.

Arribas, J., Gómez-Gras, D., Rosell, J., Tortosa, A. (1990): Estudio comparativo entre las areniscas Paleozoicas y Triásicas de la isla de Menorca: Evidencias de procesos de reciclado. *Revista de la Sociedad Geológica de España*, 3: 105-116.

Arribas, A., Mas, R., Ochoa, M., Alonso, A. (2002): Composición y diagénesis del registro detrítico en el borde suroccidental de la cuenca de Cameros. *Zubía. Instituto de Estudios Riojanos*, 14: 99-119.

Arribas, J., Alonso, A., Mas, R., Tortosa, A., Rodas, M., Barrenechea, J.F., Alonso-Azcarate, J., Artigas, R. (2003): Sandstone petrography of continental depositional sequences of a intraplate rift basin: Western Cameros Basin (North Spain). *Journal of sedimentary research*, 73 (2): 309-327.

Arribas, A., Mas, R., Arribas, M.E., Ochoa, M., González, L. (2007): Sandstone petrofacies in the Northwestern sector of the Iberian Basin. *Journal of Iberian Geology*, 33(2): 191-206.

Benito, M.I. (2001): *Estudio comparativo de la evolución sedimentaria y diagenética de los litosomas carbonatados arrecifales (pre-rifting) de la Cuenca de Cameros. Kimmeridgiense*. La Rioja- Soria. Ph.D. Thesis. Universidad Complutense de Madrid, 410 p.

Benito, M.I., Mas, R. (2001): Diagénesis temprana meteórica de la Fm. arrecifal Torrecilla en Cameros (Kimmeridgiense Inferior: prerift) y de los carbonatos de la base del Grupo Tera (Titónico: sinrift) en el sector de Soria. Cuenca de Cameros. N de España. *Geotemas*, 3(1): 83-88.

Benito, M.I., Mas, R. (2002): Evolución diagenética de los carbonatos arrecifales de la Formación Torrecilla en Cameros y de los carbonatos continentales suprayacentes (Kimmderidgiense inferior-Titónico) en el Sector de Soria. Cuenca de Cameros, N. de España. *Journal of Iberian Geology*, 28: 65-92.

Blatt, H. (1967): Provenance determination and the recycling of sediments. *Journal of Sedimentary Petrology,* 37: 1031-1044.

Chayes, F. (1952): Notes of the staining of potash feldspar with sodium cobaltonitrite in thin section. *American Mineralogist*, 37: 337-340.

Critelli, S., Le Pera, E. (1994): Detrital modes and provenance of Miocene sandstones and modern sands of the Southern Apennines thrust-top basins, Italy. *Journal of Sedimentary Research*, A64: 824-835.

Dickinson, W.R. (1970): Interpreting detrital modes of graywacke and arkose. *Journal of Sedimentary Petrology*, 40: 695-707.

Dickinson, W.R. (1985): Interpreting provenance relations from detrital modes of sandstones. In: Zuffa, G.G., ed., *Provenance of Arenites*. Dordrecht, The Netherlands, D. Reidel: 333-361.

Dickinson, W.R., Suczek, C.A. (1979): Plate tectonics and sandstone compositions: *American Association of Petroleum Geologists*, 63: 2164-2182.

Dickinson, W.R., Beard, L.S., Barkenrigge, G.R., Erjavec, J.L., Ferguson, R.C., Inman, K.F., Knepp, R.A., Lindberg, F.A., Ryberg, P.T. (1983): Provenance of North America Phanerozoic sandstones in relation to tectonic setting. *Geological Society of America Bulletin*, 94: 222-235.

Garzanti, E., Vezzoli, G., Andò, S., Castiglioni, G. (2001): Petrology of Rifted-Margin Sand (Red Sea and Gulf of Aden, Yemen). *Journal of Geology*, 109: 277-297.

Garzanti, E., Andò, S., Vezzoli, G., Dell'Era, D. (2003): From rifted margins to foreland basins: investigating provenance and sediment dispersal across desert Arabia (Oman, U.A.E.). *Journal of Sedimentary Research*, 73 (4): 572-588.

Gazzi, P. (1966): Le arenarie del flysch sopracretaceo dell'Appenino modenese; correlazioni con il flysch di Monghidoro. *Mineralogica Petrografica Acta*, 12: 69-97.

Gómez Fernández, J.C., Meléndez, N. (1994): Estratigrafía de la Cuenca de los Cameros (Cordillera Ibérica Noroccidental,

N de España) durante el tránsito Jurásico- Cretácico. *Revista Sociedad Geológica de España*, 7 (1-2): 121-139.

González-Acebrón, L. (2009): *The Tera Group in the Eastern sector of the Cameros Basin: sedimentary environments, provenance and diagenetic evolution*. Ph.D. Thesis, Universidad Complutense de Madrid, 424 p.

González-Acebrón L, Arribas J, Mas R. (2007): Provenance of fluvial sandstones at the start of late Jurassic-early Cretaceous rifting in the Cameros Basin (N. Spain). *Sedimentary Geology*, 202: 138-157.

Guimerà, J., Alonso, A., Mas, R. (1995): Inversion of an extensional-ramp basin by a newly formed thrust: the Cameros Basin (N Spain). In: Buchanan, J.G. & Buchanan, P.G. (Eds.), Basin Inversion. *Geological Society Special Publication*, 88: 433-453.

Ingersoll, R.V. (1978): Petrofacies and petrologic evolution of the Late Cretaceous forearc basin, northern and central California. *Journal of Geology*, 86: 335-352.

Ingersoll, R.V., Bulard, T.F., Ford, R.L., Grimm, J.P., Pickle, J.D., Sares, S.W. (1984): The effect of grain size on detrital modes: a text of the Gazzi- Dickinson point-counting method. *Journal of Sedimentary Petrology*, 54: 103-116.

Julivert, M. (1983): La estructura de la Zona Asturoccidental-Leonesa. In: *Geología de España*. Libro Jubilar. J.M. Ríos. Instituto Geológico y Minero de España T1: 381-407.

Julivert, M., Fontboté, J.M., Ribeiro, A., Navais Conde, L.E. (1972): *Mapa tectónico de la península Ibérica y Baleares*. E. 1: 1.000.000. Instituto Geológico y Minero de España.

Le Pera, E., Arribas, J. (2004): Sand composition in an Iberian passive-margin fluvial course: the Tajo River. *Sedimentary Geology*, 171: 261-281.

Lindholm, R.C., Finkelman, R.B. (1972): Calcite staining: semiquantitative determination of ferrous iron. *Journal of Sedimentary Petrology*, 42: 239-245.

Marcos, A. (coord.) (2004): 2.3. Zona Asturoccidental Leonesa. In: *Geología de España* (J. Vera Ed.), Sociedad Geológica de España – Instituto Geológico y Minero de España: 49-59.

Martín-Closas, M., Alonso Millán, A. (1998): Estratigrafía y Bioestratigrafía (Charophyta) del Cretácico inferior en el sector occidental de la Cuenca de Cameros (Cordillera Ibérica). *Revista de la Sociedad Geológica de España*, 11: 253-269.

Martínez-Catalán, J.R. (coord.) (2004): Zona Centroibérica. In: *Geología de España* (J. Vera Ed.), Sociedad Geológica de España – Instituto Geológico y Minero de España: 68-83.

Mas, R., Alonso, A., Guimerà, J. (1993): Evolución tectonosedimentaria de una cuenca extensional intraplaca: la cuenca finijurásica- eocretácica de Los Cameros (La Rioja-Soria). *Revista Sociedad Geológica de España*, 6 (3-4): 129-144.

Mas, R., Benito, M.I.; Arribas, J., Serrano, A., Guimerà, J., Alonso, A., Alonso-Azcarate, J. (2002): La Cuenca de Cameros: desde la extensión finijurásica-eocretácica a la inversión terciaria – implicaciones en la exploración de hidrocarburos. *Zubía*. Instituto de Estudios Riojanos, 14: 9-64.

Mas, R., Benito, M.I., Arribas, J., Serrano, A., Alonso, A., Alonso-Azcarate, J. (2003): The Cameros Basin: From Late Jurassic- Early Cretaceous Extension to Tertiary Contractional Inversion- Implications of Hydrocarbon Exploration. In: *AAPG International Conference and Exhibition*, Barcelona, Spain. Geological Field Trip 11, 52 pages.

Mas, R. (coord.), García, A (coord.), Salas, R., Meléndez, A., Alonso, A., Aurell, M., Bádenas, B., Benito, M.I., Carenas, B., García-Hidalgo, J.F., Gil, J., Segura, M., (2004): 5.3.3. Segunda fase de rifting: Jurásico Superior-Cretácico Inferior. In: *Geología de España* (J. Vera Ed.), Sociedad Geológica de España – Instituto Geológico y Minero de España: 503-509.

Palomares, M., Arribas, J. (1993): Modern stream sands from compound crystalline sources: Composition and sand generation index. In: Johnsson, M.J. & Basu, A., Eds. Processes Controlling the Composition of Clastic Sediments. *Geological Society of America, Special Paper*, 284: 313-322.

Pettijohn, F.J., Potter, P.E., Siever, R. (1972): Sand and sandstones. Springer - Verlag, New York – Heidelberg – Berlín, 618 p.

Salas, R., Guimerá, J., Mas, R., Martín-Closas, C., Meléndez, A., Alonso, A., 2001. Evolution of the Mesozoic Central Iberian Rift System and its Cainozoic Inversion (Iberian Chain). In: Peri-Tethyan Rift- Wrench Basins and Passive Margins (Eds. W. Cavazza, A.H.F.R. Roberson and P. Ziegler). *Mémoires du Muséum National d'Histoire Naturelle, 186*: 145-185.

Shanley, K.W., McCabe, P.J., 1995. Sequence stratigraphy of Turonian-Santonian strata, Kaiparowits Plateau, southern Utah, USA - implications for regional correlation and foreland basin evolution. In: Van Wagoner, JC, Bertram G. (eds). Sequence Stratigraphy of Foreland Basin Deposits - Outcrop and Subsurface Examples from the Cretaceous of North America. AAPG Memoir 64. Pp. 103-136.

Tyrell, S., Haughton, P.D.W., Daly, J.S. (2007): Drainage reorganization during breakup of Pangea revealed by in-situ Pb isotopic analysis of detrital K-feldspar. *Geology*, 35: 971-974.

Valloni, R. (1985): Reading provenance from modern marine sands. In: Zuffa. G.G., Ed., *Provenance of Arenites*. The Netherlands, Dordrecht, Reidel, 309-332.

Villaseca, C., Barbero, L., Huertas, M.J., Andonaegui, P., Bellido, F. (1993): A cross-section though Hercynian granites of the Central Iberian Zone, Excursion guide, Servicio de Publicaciones, Consejo Superior de Investigaciones Científicas, Madrid, pp. 122.

Zuffa, G.G. (1980): Hybrid arenites: their composition and classification. Journal of Sedimentary Petrology, 50: 21-29.

Zuffa, G.G. (1985): Optical analyses of arenites: influence of methodology on compositional results, in Zuffa, G.G., ed., *Provenance of arenites*: The Netherlands, Dordrecht, Reidel: 165-189.

Zuffa, G.G., 1987. Unravelling hinterland and offshore palaeogeography from deep-water arenites. In: Marine Clastic Sedimentology, Chapter 2, 39-61.